SOLAR ENERGY

THE JOURNAL OF SOLAR ENERGY SCIENCE AND ENGINEERING

VOLUME IV JULY, 1960 NUMBER 3

PUBLISHED QUARTERLY BY THE ASSOCIATION FOR APPLIED SOLAR ENERGY ARIZONA STATE UNIVERSITY, TEMPE, ARIZONA

SUBSCRIPTIONS

The Journal is sent to AFASE members as one of their membership benefits. Nonmembers may purchase single copies of this issue at $3 per copy, or may obtain a subscription at $10 per year. Please send all communications and inquiries regarding back numbers, dues, etc., to AFASE at the above address. All correspondence regarding manuscripts should be addressed to A. B. Stafford, Arizona State University.

TABLE OF CONTENTS

Cover Photo: Picture by Joseph Muench

Sunset Over the North Rim. Looking from Crazy Jug Point on the North Rim of the Grand Canyon into a brilliant sunset that illuminates the clouds. Grand Canyon Nat'l Park, Ariz.

SOLAR ENERGY

THE JOURNAL OF SOLAR ENERGY SCIENCE AND ENGINEERING

VOLUME IV JULY, 1960 NUMBER 3

PUBLISHED QUARTERLY BY THE ASSOCIATION FOR APPLIED SOLAR ENERGY ARIZONA STATE UNIVERSITY, TEMPE, ARIZONA

SUBSCRIPTIONS

The Journal is sent to AFASE members as one of their membership benefits. Nonmembers may purchase single copies of this issue at $3 per copy, or may obtain a subscription at $10 per year. Please send all communications and inquiries regarding back numbers, dues, etc., to AFASE at the above address. All correspondence regarding manuscripts should be addressed to A. B. Stafford, Arizona State University.

TABLE OF CONTENTS

Cover Photo: Picture by Joseph Muench

Sunset Over the North Rim. Looking from Crazy Jug Point on the North Rim of the Grand Canyon into a brilliant sunset that illuminates the clouds. Grand Canyon Nat'l Park, Ariz.

The Interrelationship and Characteristic Distribution of Direct, Diffuse and Total Solar Radiation*

By Benjamin Y. H. Liu† and Richard C. Jordan‡

Based upon the data now available, this paper presents relationships permitting the determination on a horizontal surface of the instantaneous intensity of diffuse radiation on clear days, the long term average hourly and daily sums of diffuse radiation, and the daily sums of diffuse radiation for various categories of days of differing degrees of cloudiness. For these determinations, it is necessary to have, either from actual measurements or estimates, a knowledge of the total (direct plus diffuse) radiation on a horizontal surface—its measurement is now regularly made at 98 localities in the United States and Canada. For localities where only an estimate of the long term average total radiation is available, relationships presented in this paper can be utilized to determine the statistical distribution of the daily total radiation at these localities.

NOMENCLATURE

D and $\bar{D}$ = daily and monthly average daily diffuse radiation received on a horizontal surface, Btu/day-sq ft

f = fractional time during which the daily total radiation received on a horizontal surface is less than or equal to a certain value, dimensionless

H and $\bar{H}$ = daily and monthly average daily total (direct plus diffuse) radiation received on a horizontal surface, Btu/day-sq ft

H_o = extraterrestrial daily insolation received on a horizontal surface, Btu/day-sq ft

I_{Dh} = intensity of direct radiation incident upon a horizontal surface, Btu/hr-sq ft

I_{Dn} = intensity of direct radiation at normal incidence, Btu/hr-sq ft

I_{dh} = intensity of diffuse radiation on a horizontal surface, Btu/hr-sq ft

$\bar{I}_{dh}$ = long term average of the hourly diffuse radiation received on a horizontal surface = long term hourly average of the intensity of diffuse radiation on a horizontal surface, Btu/hr-sq ft

I_{oh} = intensity of solar radiation incident upon a horizontal surface outside the atmosphere of the earth, Btu/hr-sq ft

I_{on} = intensity of solar radiation at normal incidence outside the atmosphere of the earth = rI_{sc}, Btu/hr-sq ft

I_{sc} = solar constant = 442 Btu/hr-sq ft = 2 ly/min

I_{Th} = intensity of total (direct plus diffuse) radiation incident upon a horizontal surface, Btu/hr-sq ft

$\bar{I}_{Th}$ = long term average of the hourly total radiation received on a horizontal surface = long term hourly average of the intensity of total radiation on a horizontal surface, Btu/hr-sq ft

K_d and $\bar{K}_d$ = D/H_o and $\bar{D}/H_o$, dimensionless

K_D = $(H - D)/H_o$, dimensionless

K_T and $\bar{K}_T$ = H/H_o and $\bar{H}/H_o$, dimensionless

L = latitude, degrees

m = air mass = $csc\alpha$ except at low altitude, dimensionless

r = ratio of solar radiation intensity at normal incidence outside the atmosphere of the earth to solar constant, dimensionless

r_d = $\bar{I}_{dh}/\bar{D}$ = ratio of hourly to daily diffuse radiation, dimensionless

r_T = ratio of hourly to daily total radiation, dimensionless

α = solar altitude angle, degrees

δ = solar declination, degrees

τ_D = $I_{Dn}/I_{on} = I_{Dh}/I_{oh}$ = transmission coefficient for direct solar radiation, dimensionless

τ_d = I_{dh}/I_{oh} = transmission coefficient for

---

* This paper is in part the result of researches sponsored by a grant from the National Science Foundation, Washington, D. C. Portions of the material presented in this paper are drawn from the thesis of Benjamin Y. H. Liu prepared in partial fulfillment of the requirements of the degree of Doctor of Philosophy.

† Assistant Professor, Department of Mechanical Engineering, University of Minnesota.

‡ Professor and Head, Department of Mechanical Engineering, University of Minnesota.

Table 1.—Solar Declination, δ, and the ratio, r, of Solar Radiation Intensity at Normal Incidence Outside Earth's Atmosphere to Solar Constant

Month	Day of Month							
	1		8		15		22	
	δ	r	δ	r	δ	r	δ	r
January	−23°04′	1.0335	−22°21′	1.0325	−21°16′	1.0315	−19°51′	1.0300
February	−17°19′	1.0288	−15°14′	1.0263	−12°56′	1.0235	−10°28′	1.0207
March	−7°53′	1.0173	−5°11′	1.0140	−2°26′	1.0103	0°20′	1.0057
April	4°15′	1.0009	6°55′	0.9963	9°30′	0.9913	11°56′	0.9875
May	14°51′	0.9841	16°53′	0.9792	18°41′	0.9757	20°14′	0.9727
June	21°57′	0.9714	22°47′	0.9692	23°17′	0.9680	23°27′	0.9670
July	23°10′	0.9666	22°34′	0.9670	21°39′	0.9680	20°26′	0.9692
August	18°13′	0.9709	16°22′	0.9727	14°18′	0.9757	12°03′	0.9785
September	8°34′	0.9828	5°59′	0.9862	3°20′	0.9898	0°37′	0.9945
October	−2°54′	0.9995	−5°36′	1.0042	−8°14′	1.0087	−10°47′	1.0133
November	−14°11′	1.0164	−16°21′	1.0207	−18°18′	1.0238	−19°58′	1.0267
December	−21°41′	1.0288	−22°39′	1.0305	−23°14′	1.0318	−23°27′	1.0327

diffuse radiation on a horizontal surface, dimensionless

τ_T = I_{Th}/I_{oh}, = transmission coefficient for total radiation on a horizontal surface, dimensionless

ω = hour angle, degrees

ω_s = sunset hour angle, radians

INTRODUCTION

The increase in recent years of the problems with which solar radiation is involved has made solar radiation information frequently needed by workers in many fields. Although solar radiation data are now available for many localities, difficulties are sometimes encountered in utilizing these data since they consist primarily of total (direct plus diffuse) radiation only and a knowledge of the diffuse component is often required. Since the theoretical computation of diffuse radiation is extremely difficult if not impossible at the present time, an attempt is made in this study to investigate, from the limited data now available, the relationships between diffuse and total radiation in order that they may be utilized for the estimation of diffuse radiation for localities where only the total radiation is known. This was first attempted by Parmelee[1] for cloudless days only, but no extension was made to cloudy days.

In this investigation it has also been found necessary to study the characteristic distribution of total radiation. The results obtained serve to indicate the types of parameters to be used in the investigation of other statistical characteristics of solar radiation should the need for these characteristics arise. The present study is restricted to radiation on a horizontal surface only.

Solar Constant

Since a definite value for the solar constant must be used consistently throughout this study, the most recent value of 2.00 ly/min,* or 442 Btu/hr-sq ft, given by Johnson,[2] in terms of the Smithsonian Pyrheliometric Scale of 1932† shall be adopted. The solar constant is the rate at which solar energy is impinging upon a unit surface, normal to sun's rays, in free space, at the earth's mean distance from the sun. It is in general slightly different from the solar radiation at normal incidence at the outer limit of the atmosphere due to the variation of the distance between the earth and the sun. (See Table 1.)

Relationships Between the Intensities of Direct and Diffuse Radiation on Clear Days

As solar radiation penetrates the atmosphere it is depleted by absorption and scattering. Not all of the scattered radiation is lost, since part of it eventually arrives at the surface of the earth in the form of diffuse radiation. The term, diffuse radiation, is used here in the customary way to denote this short wavelength radiation coming from all parts of the sky. It should be distinguished clearly from the atmospheric thermal radiation which, although also diffuse in nature, is of much longer wavelengths.

To facilitate the discussion, the following dimensionless transmission coefficients shall be defined:

τ_D = transmission coefficient for direct solar radiation $= I_{Dn}/I_{on} = I_{Dh}/I_{oh}$

τ_d = transmission coefficient for diffuse radiation on a horizontal surface $= I_{dh}/I_{oh}$

These transmission coefficients are functions of the solar altitude, atmospheric water vapor content, dust content, ozone content, and any other radiation de-

* 1.0 langley/min = 1.0 gm cal/min-sq cm = 3.687 Btu/min-sq ft = 69.7 milliwatts/ sq cm.

† The 1932 Pyrheliometric Scale of the Smithsonian Institution is 2.5% below the scale of 1913, 1.0% above the Angstrom scale and 0.5% below the recently proposed International Pyrheliometric Scale.[3]

pleting factors. However, in a nonindustrial locality where the atmosphere is relatively clean and the effect of dust small, the daily variation of these transmission coefficients for the sun at a fixed altitude, is primarily due to the variation of the atmospheric water vapor. Thus as the atmospheric water vapor content varies from day to day causing both τ_D and τ_d to vary, a functional relationship between τ_D and τ_d is generated.

The four upper curves of Fig. 1 show the theoretical relationships between τ_D and τ_d for a cloudless and dust free atmosphere for four air masses, 1, 2, 3 and 4 corresponding to solar altitude angles of 90, 30, 19.5 and 14.5 respectively. These relationships can be derived readily from the transmission coefficients computed by Kimball when the assumption is made that the diffuse radiation received on a horizontal surface is half of the solar radiation scattered by the atmospheric constituents.[4] However, due to the fact that Kimball's computations are based upon a zero air mass solar spectrum low in the ultraviolet, the theoretical values of τ_D and τ_d in Fig. 1 have been reduced by 3%. Since these theoretical relationships have been derived without considering the effect of dust and are based upon an assumption which is known to be only approximately correct, they should not be expected to represent the correct relationships between τ_D and τ_d under actual cloudless sky conditions and are derived here to serve merely as guides in the search of experimental relationships.

The experimental points of Fig. 1 are derived from the measurements made at Hump Mountain, North Carolina, by Moore and Abbot[5] whose data appear to be the best available. In computing the experimental transmission coefficients, however, the direct and diffuse radiation intensities from the original data have been reduced by 2.5% in order that the radiation intensities be expressed in the 1932 Smithsonian Pyrheliometric scale upon which the presently adopted solar constant of 2.00 ly/min is based.

The fact that both the theoretical curves and experimental points of Fig. 1 show that the values of τ_d corresponding to a fixed value of τ_D depend only very moderately upon the air mass indicates that, for the degree of accuracy here sought, a relationship which is independent of the air mass is adequate. The following equation of a straight line, obtained by the method of least squares, best fits the experimental points:

$$\tau_d = 0.2710 - 0.2939\tau_D \qquad [1]$$

A total of 149 points representing the data of 28 clear days were used in obtaining this equation. The probable error computed by the equation,

$$\text{Probable error} = 0.6745 \sqrt{\frac{v^2}{n-1}}$$

is 0.0052, where v is the difference between the experimental value of τ_d and the value of τ_d given by the straight line at the same value of τ_D, and n the total number of points used.

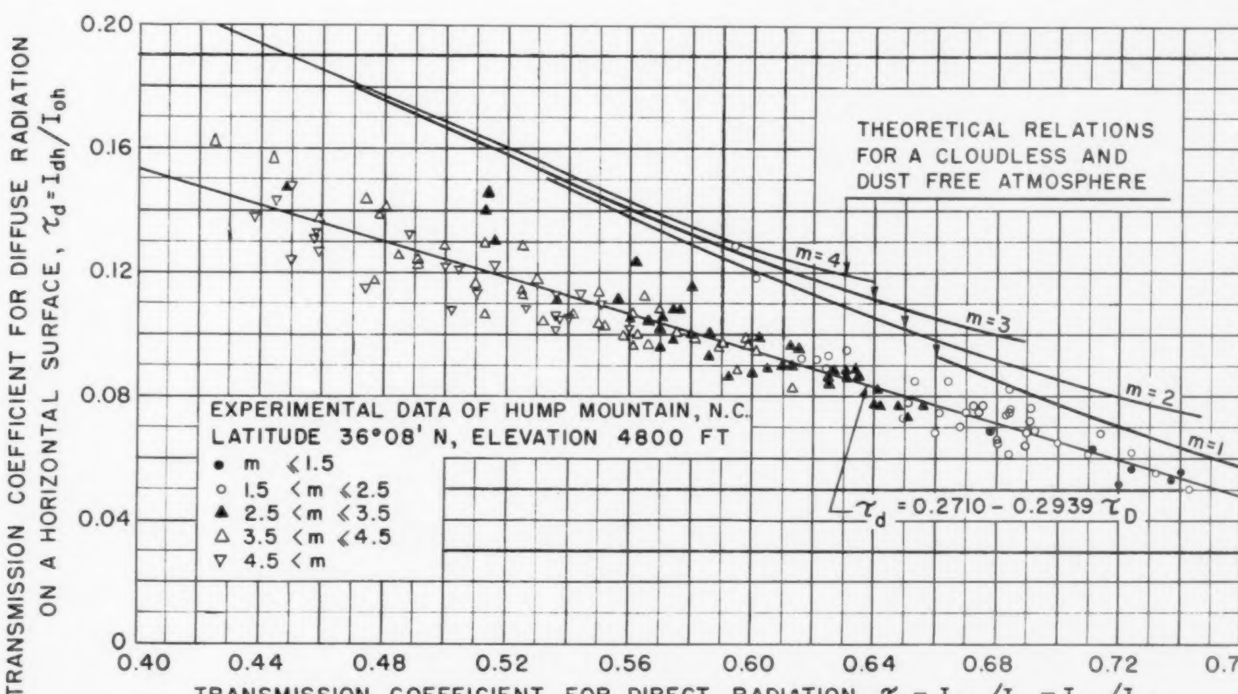

FIG. 1—Theoretical and experimental relations between the intensities of direct and diffuse radiation on a horizontal surface for a cloudless atmosphere at 4800 ft elevation.

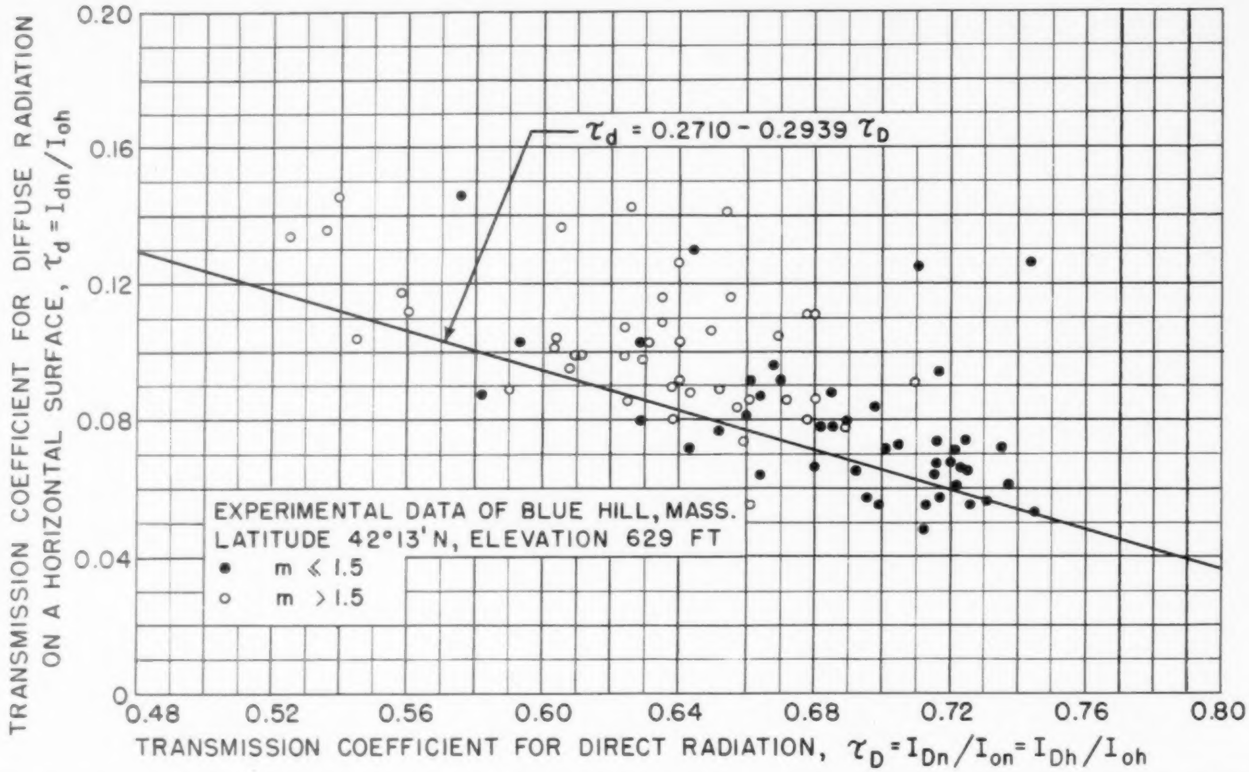

FIG. 2—Comparison of the empirical relation between the intensities of direct and diffuse radiation on a horizontal surface derived from the data for Hump Mountain, N. C., with the data for Blue Hill, Mass.

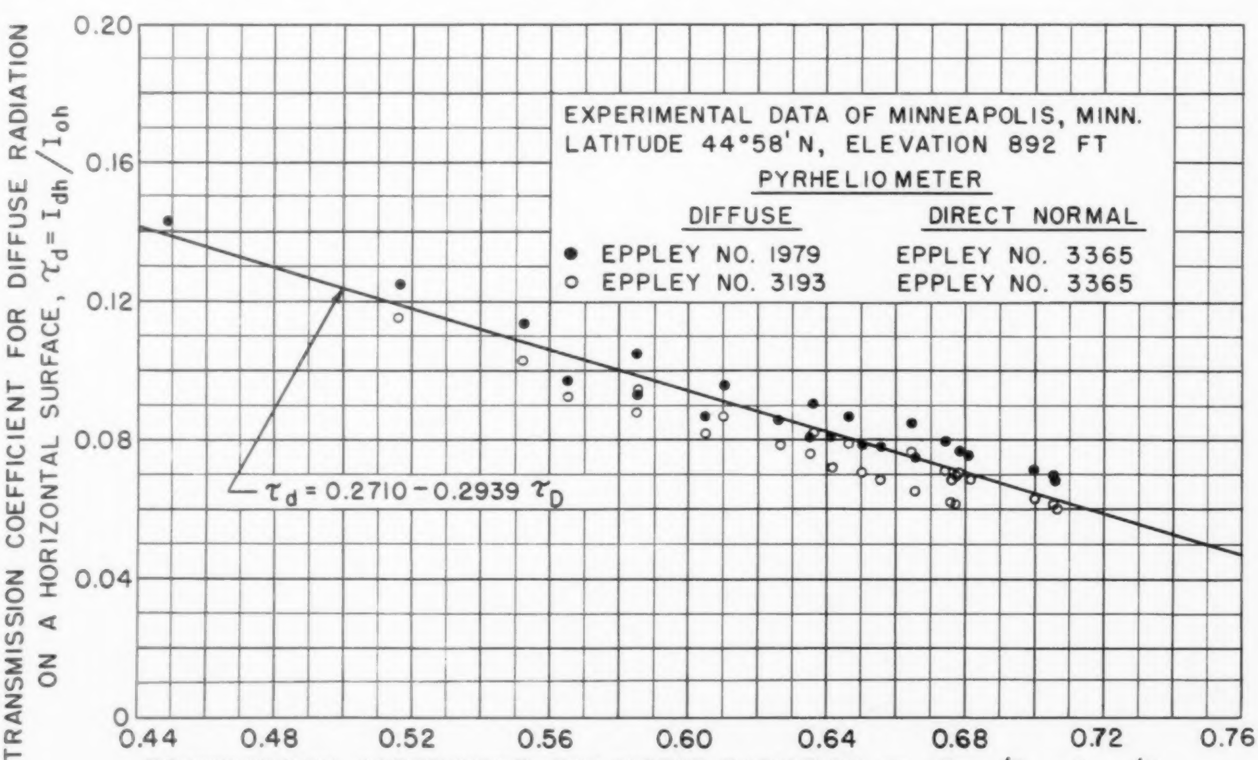

FIG. 3—Comparison of the empirical relation between the intensities of direct and diffuse radiation on a horizontal surface derived from the data for Hump Mountain, N. C., with the data for Minneapolis, Minn.

The reasons that the observed diffuse radiation values are lower than the theoretical values computed for a dust free atmosphere, under the assumption that half of the scattered radiation reaches the earth's surface, are not immediately apparent. Since the theoretical relationships do not take into consideration the effects of dust and since an atmosphere is never completely dust free, the observed diffuse radiation intensities would be expected to be higher than those predicted if the usual assumption is made that dust particles scatter but do not absorb radiation.[4,6] The effect of terrain reflection which was not considered in obtaining the theoretical relationships would also tend to increase the diffuse radiation, since the radiation thus reflected is in turn scattered by the atmospheric constituents and a fraction of this scattered radiation again arrives at the earth's surface. Furthermore, the assumption that half of the scattered radiation reaches the earth's surface is true for pure Rayleigh scattering by air molecules only. The more intensely forward scattered components usually associated with water vapor scattering probably should increase the observed diffuse radiation intensity to values even greater than those predicted. Therefore, it appears that in travelling toward the earth's surface a substantial fraction of the scattered radiation must have been absorbed by the atmospheric water vapor or other absorbing media in the atmosphere. Nevertheless, this factor alone does not seem to have an effect of sufficient magnitude to account for the differences between the theoretical and experimental diffuse radiation intensities, as shown in Fig. 1. However, regardless of the reasons for this difference, Equation [1] provides a means for estimating the intensity of diffuse radiation on a horizontal surface under a cloudless atmosphere when the intensity of direct radiation at normal incidence is known. Since the intensity of total radiation on a horizontal surface is the sum of the intensities of direct and diffuse radiation on a horizontal surface, the following relation between τ_d and τ_T can be readily derived from Equation [1]

$$\tau_d = 0.3840 - 0.4160\tau_T \qquad [2]$$

where τ_T is the ratio of the intensity of total radiation on a horizontal surface to the intensity of radiation incident upon a horizontal surface on top of the atmosphere.

To test whether Equation [1] also represents the correct relationship between the intensities of direct and diffuse radiation at localities other than Hump Mountain, it has been compared with the data of Hand[7] for Blue Hill, Massachusetts, and measurements made by the authors at the University of Minnesota, Minneapolis, Minnesota. These are shown in Figs. 2 and 3. Even though the data for Blue Hill show considerable scattering and the diffuse radiation measurements are higher than those for Hump Mountain, the agreement is still quite satisfactory. The agreement of Equation [1] with the experimental data for Minneapolis is extremely good and the small differences are entirely within the experimental uncertainties of the diffuse radiation measurements by the Eppley pyrheliometers. (Examination of Fig. 3 shows that diffuse radiation measured by two different Eppley pyrheliometers differ by about 10%.) Therefore, it is felt that Equation [1] and hence Equation [2] are of general validity and should be applicable to many localities where the albedo (reflectivity) of the surrounding terrain and the atmospheric contamination by dust are not greatly different from those at Hump Mountain, Blue Hill, and Minneapolis.

Relationship Between Daily Diffuse and Daily Total Radiation on Cloudy Days

Due to the extremely variable cloudiness the intensities of direct and diffuse radiation under sky conditions not completely cloudless will also be highly variable and their values at any one instant are impossible to predict. Therefore, any attempt to establish a relationship between diffuse radiation and total radiation during cloudy days must involve statistical averages which can be obtained from experimental data covering a sufficiently long period of time.

If one month is taken as a period during which the solar declination does not vary excessively, and consequently the daily solar radiation incident upon a horizontal surface outside the atmosphere at a locality also remains fairly constant, then during a month the day to day variation of the daily total and daily diffuse radiation received on a horizontal surface at a locality is primarily due to the variation of cloudiness, and to much lesser extents, the variation of the atmospheric water vapor, dust, and ozone contents. Since the amount of total radiation received on a horizontal surface during a day is an indication of the degree of atmospheric cloudiness whose variability is largely responsible for the observed diffuse radiation variations from day to day, it is expected that, when suitable statistical averages are taken, a relationship will exist between the daily total and daily diffuse radiation for each month at a given locality.

Fig. 4 shows such relationships derived from the ten year (1947–1956) data for Blue Hill, Massachusetts,[8] for the three months, December, March and June. The value of the daily diffuse radiation, D, at each point in Fig. 4 is the average of the daily diffuse radiation received on days with daily total radiation equal to H. However, due to the fact that the number of days with exactly equal values of daily total radiation is extremely small even within the same month, the value of H at

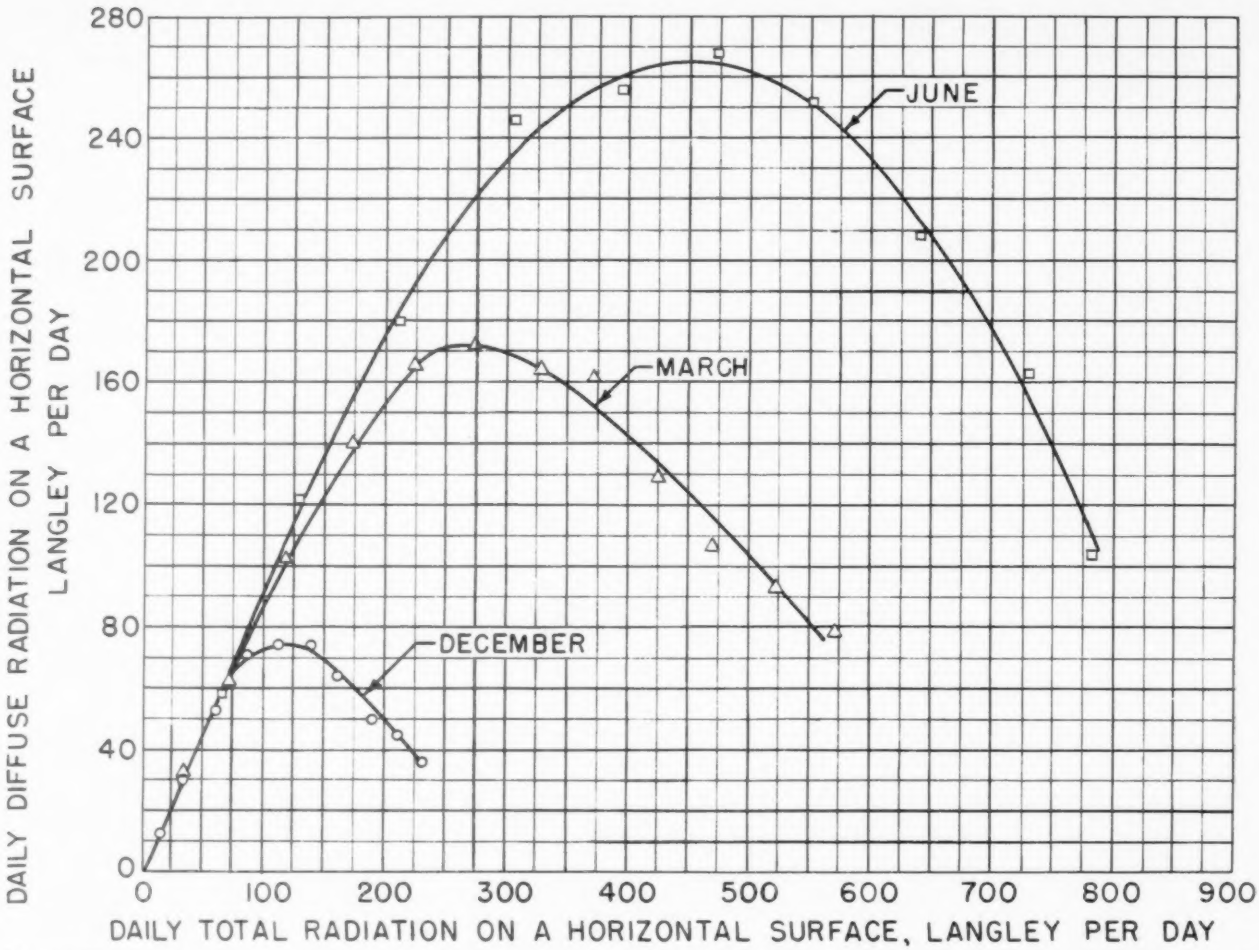

FIG. 4—The relation between the daily total radiation and daily diffuse radiation on a horizontal surface for December, March and June at Blue Hill, Mass.

each point in Fig. 4 is actually the average of the daily total radiation for days whose daily total radiation fall within a small interval of values (the size of the interval is indicated by the difference in the values of H of the neighboring points in Fig. 4). Since ten year data for each month are used and approximately ten points are obtained for each month, each point in Fig. 5 represents approximately the average of thirty days.

The results of Fig. 5 show that a fairly smooth relationship exists between the daily diffuse and daily total radiation for each of the three months. Furthermore, the similarities between the forms of the three curves indicate the possibility of obtaining a unique representation of these relations through normalizing the coordinates. That this indeed is the case can be seen by referring to Fig. 5 showing the relationship between the daily diffuse and daily total radiation for the entire twelve months in the normalized coordinates K_d and K_T where

$$K_d = D/H_o \quad [3]$$

$$K_T = H/H_o \quad [4]$$

and H_o, the extraterrestrial daily insolation received on a horizontal surface, is computed from the following equation

$$H_0 = \frac{24}{\pi} rI_{sc}(\cos L \cos \delta \sin \omega_s + \omega_s \sin L \sin \delta) \quad [5]$$

with the use of the mean solar declination for each month. The sunset hour angle, ω_s, i.e. the hour angle at which the sun sets in the west, in Equation [5] can be determined as follows:

$$\cos \omega_s = -\tan L \tan \delta \quad [6]$$

The solar declination for the selected days of each month and the ratio, r, of the intensity of radiation at normal incidence outside the atmosphere to the solar constant are given in Table 1. A graphical representation of Equation [6] is shown in Fig. 6 with H_o plotted against the latitude and with the month as a parameter.

Despite a more than threefold increase in the value of H_o from December to June at the latitude (42°13′N) of Blue Hill, as an examination of Fig. 6 will show, the results of Fig. 5 show that a fairly definite relationship

exists between the two dimensionless quantities K_d and K_T. It is of interest to note that on days which are relatively cloud free ($K_T = 0.75$) the diffuse radiation received on a horizontal surface is approximately 12% ($K_d = 0.12$) of the solar radiation outside the atmosphere. On certain partly cloudy days ($K_T = 0.40$), however, the diffuse radiation is over twice the clear day value and reaches as much as 25% of the extraterrestrial insolation. With increasing cloudiness, as K_T approaches zero, K_d also approaches zero as would be expected.

The curves of Fig. 5 thus offer an interesting possibility for a method of estimating, to an average accuracy of approximately ±5%, the daily diffuse radiation at localities where measurements of daily total radiation are made, provided, of course, that the relationships of Fig. 5 also hold for other localities. Since additional data is sparse, it has not been possible to extend the studies to other locations. However, it will be shown in subsequent developments that the results derived assuming the validity of these results continue to compare favorably with all available experimental evidence.

A special comment is needed for the few points with $K_T > 0.75$ as they appear to deviate from the general trend of the other points. It should be recalled that in Equations [3] and [4], H_o was computed using the average solar declination for each month. Thus the values of K_T (or K_d) for each point in Fig. 5 truly represent the fraction of the extraterrestrial daily insolation transmitted through the atmosphere as total radiation (or as diffuse radiation), and thus accurately provide an indication of the degree of cloudiness, only if the value of H_o so computed is the true average of the extraterrestrial insolation for the days whose data are used in obtaining each point. Since the extraterrestrial daily insolation does vary to some extent during a month, this then requires that the days whose data are used to obtain a point distribute themselves symmetrically with respect to the middle of the month. In analyzing the data for Blue Hill it was found that this requirement is nearly obeyed for all points with $K_T < 0.75$ but not for the few points with $K_T > 0.75$. In fact the large values of K_T for these points are direct consequences for the fact that the values of H_o used are smaller than the true average. A much better

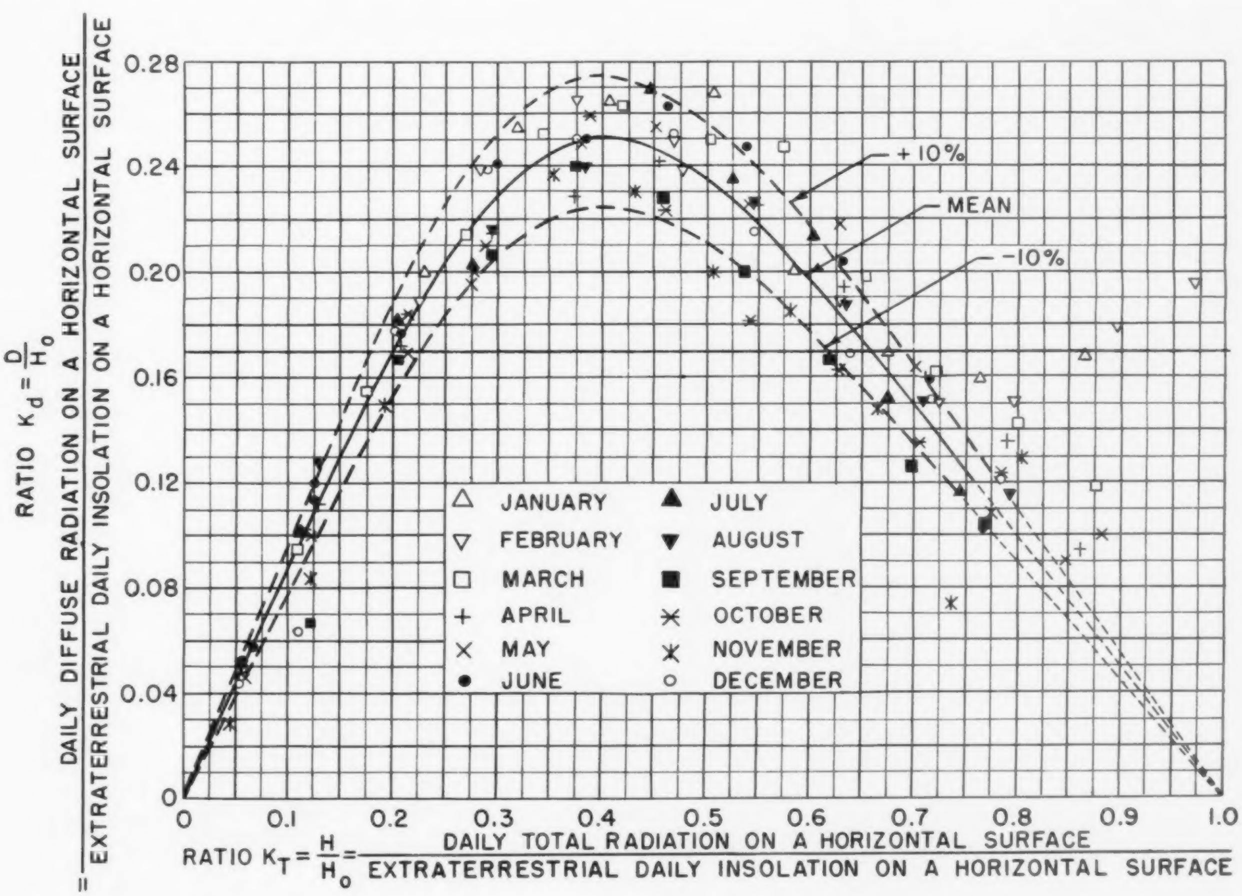

Fig. 5—The relation between the daily total radiation and daily diffuse radiation on a horizontal surface.

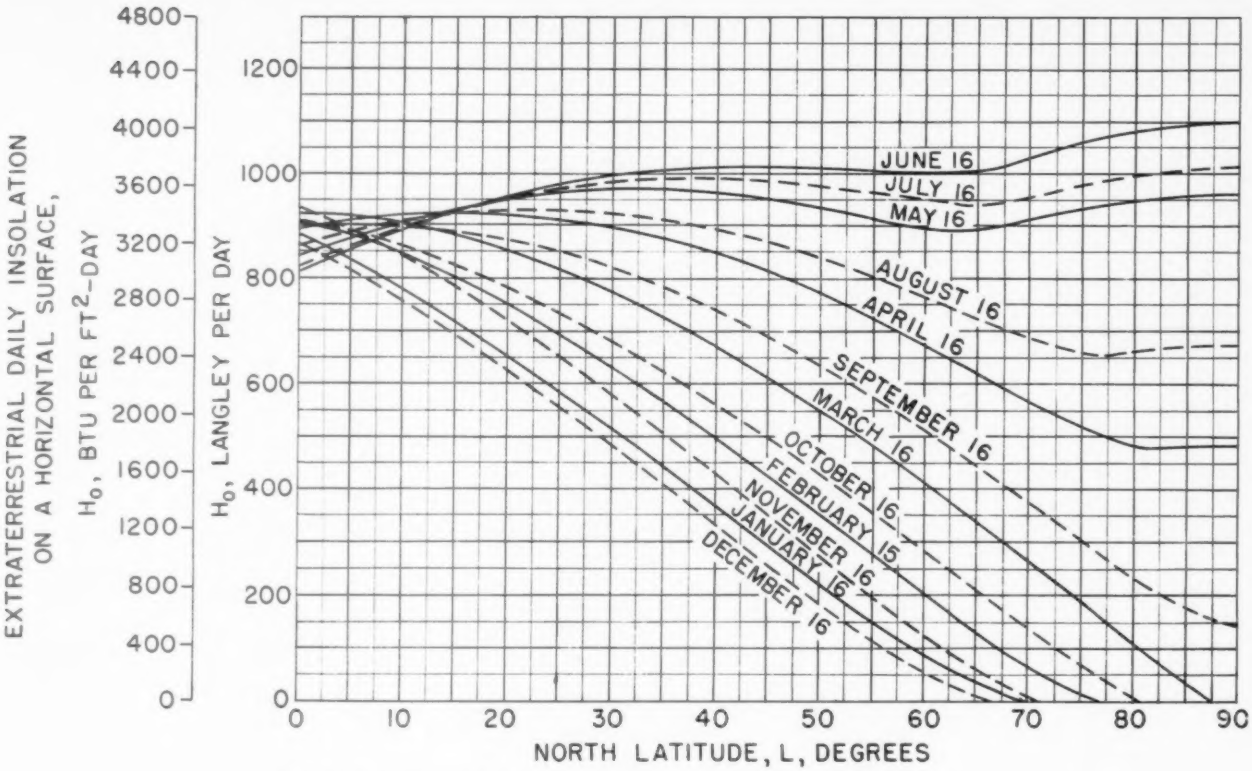

FIG. 6—Extraterrestrial daily insolation received on a horizontal surface.

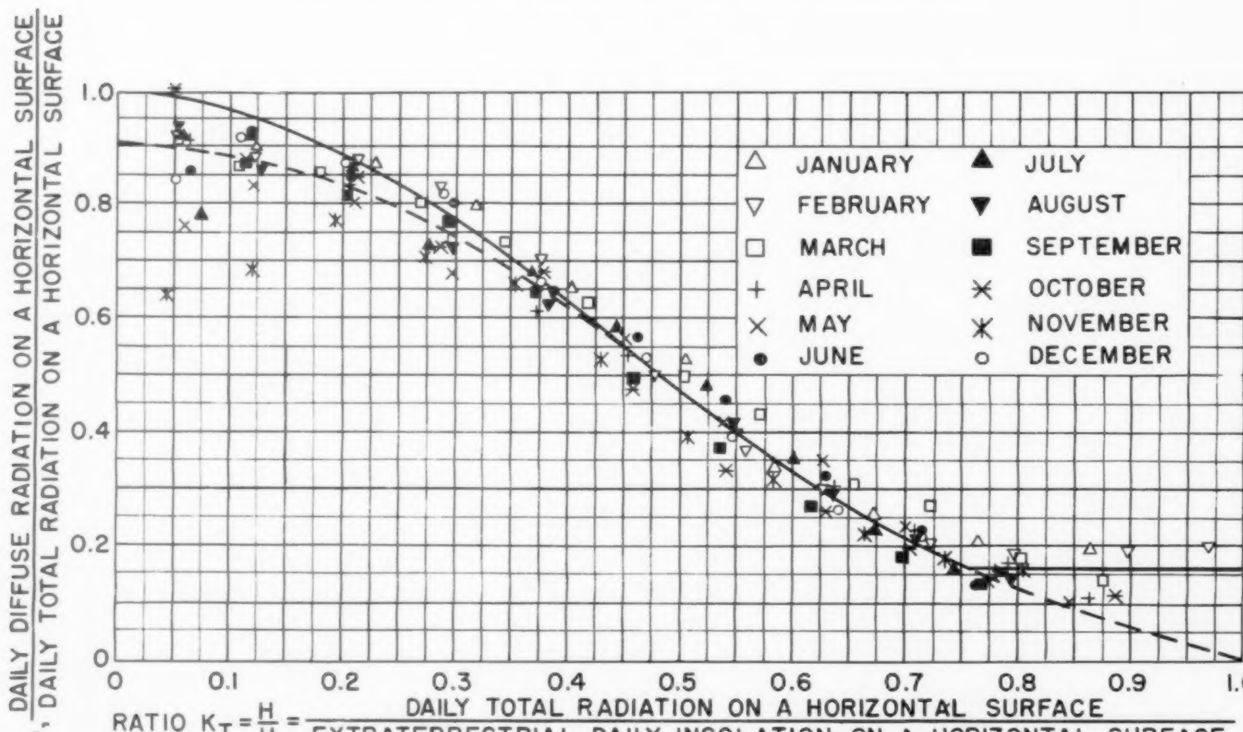

FIG. 7—The ratio of the daily diffuse radiation to the daily total radiation as a function of the cloudiness index K_T.

VOL. 4 1960

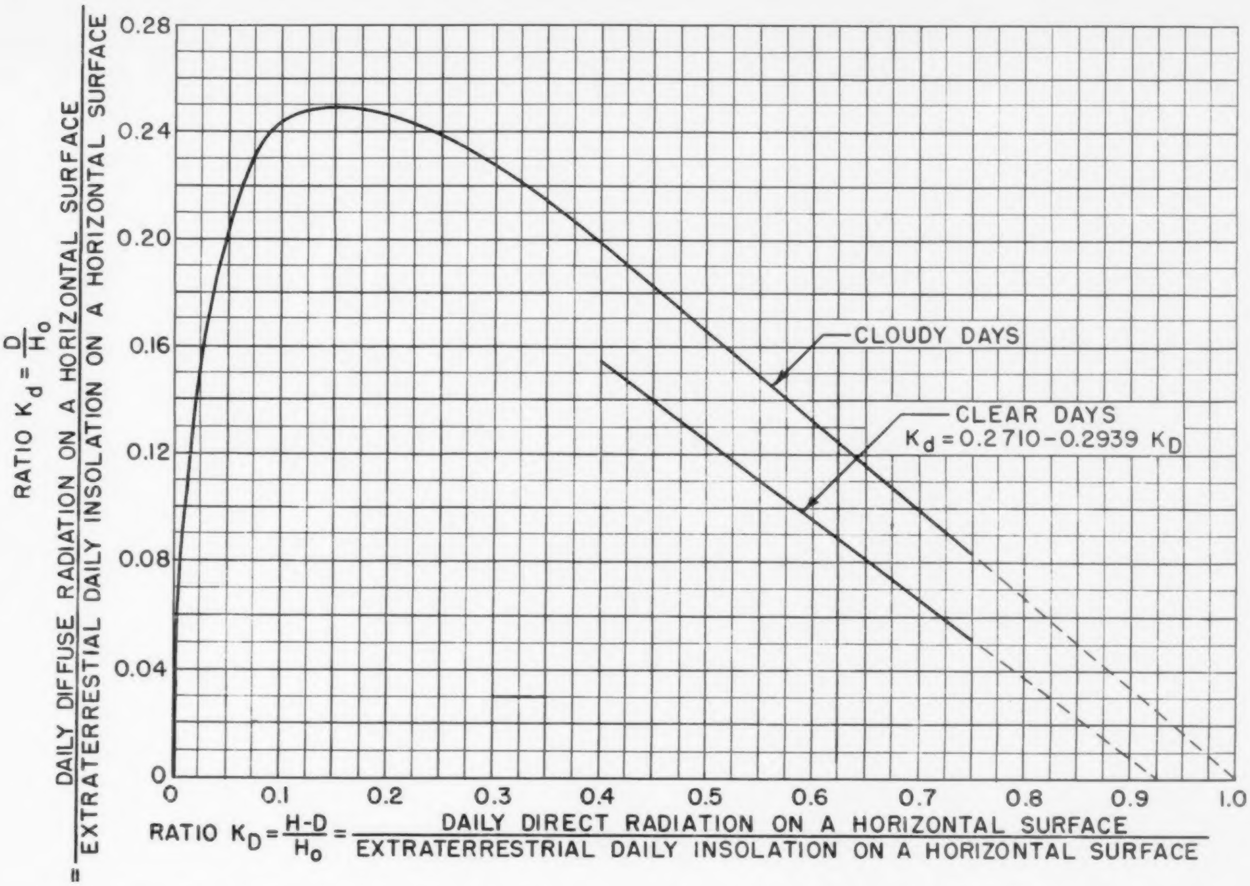

FIG. 8—Comparison of the relations between the daily direct radiation and the daily diffuse radiation on a horizontal surface on clear and cloudy days.

result would have been obtained had the "correct" average H_o been employed. This was not done in order that H_o for each month might have a definite value. To overcome this difficulty it is recommended that when $K_T > 0.75$ the average ratio 0.16 of D/H for these points be used.

The ratio D/H is shown as a function of K_T in Fig. 7. Since the diffuse and total radiation should be equal for completely overcast days, the ratio D/H should approach the limit one when K_T approaches zero. An inconsistency in the data is seen for the points with values of K_T near zero. The solid curve is so drawn that the ratio D/H is brought to unity when K_T equals zero, and it is recommended that this curve be used for practical application.

Comparison of the Clear and Cloudy Day Relationships Between the Daily Direct and Diffuse Radiation

A comparison between the clear and cloudy day diffuse radiation is shown in Fig. 8 where K_d of Fig. 5 is plotted against K_D with

$$K_D = (H - D)/H_o = K_T - K_d \qquad [7]$$

and represents the fraction of the extraterrestrial daily insolation transmitted through the atmosphere as direct radiation. Since K_d and K_D are respectively the weighed averages of τ_d and τ_D, and since on clear days the relation between τ_d and τ_D is linear, when K_d and K_D are substituted for τ_d and τ_D in Equation [1], an equation is obtained which represents the relationship between the daily direct and diffuse radiation received on a horizontal surface on clear days. Thus, on clear days,

$$K_d = 0.2710 - 0.2939 K_D \qquad [8]$$

which is also plotted in Fig. 8.

The effects of clouds on diffuse radiation is clearly seen from Fig. 8 which shows that the value of K_d on cloudy days is higher than the corresponding value of K_d on clear days at the same values of K_D. The higher diffuse radiation on cloudy days is obviously due to the additional scattering effects of clouds.

Statistical Distribution of the Daily Total Radiation on a Horizontal Surface

In the majority of cases it is more important to have a knowledge of the monthly average of the daily dif-

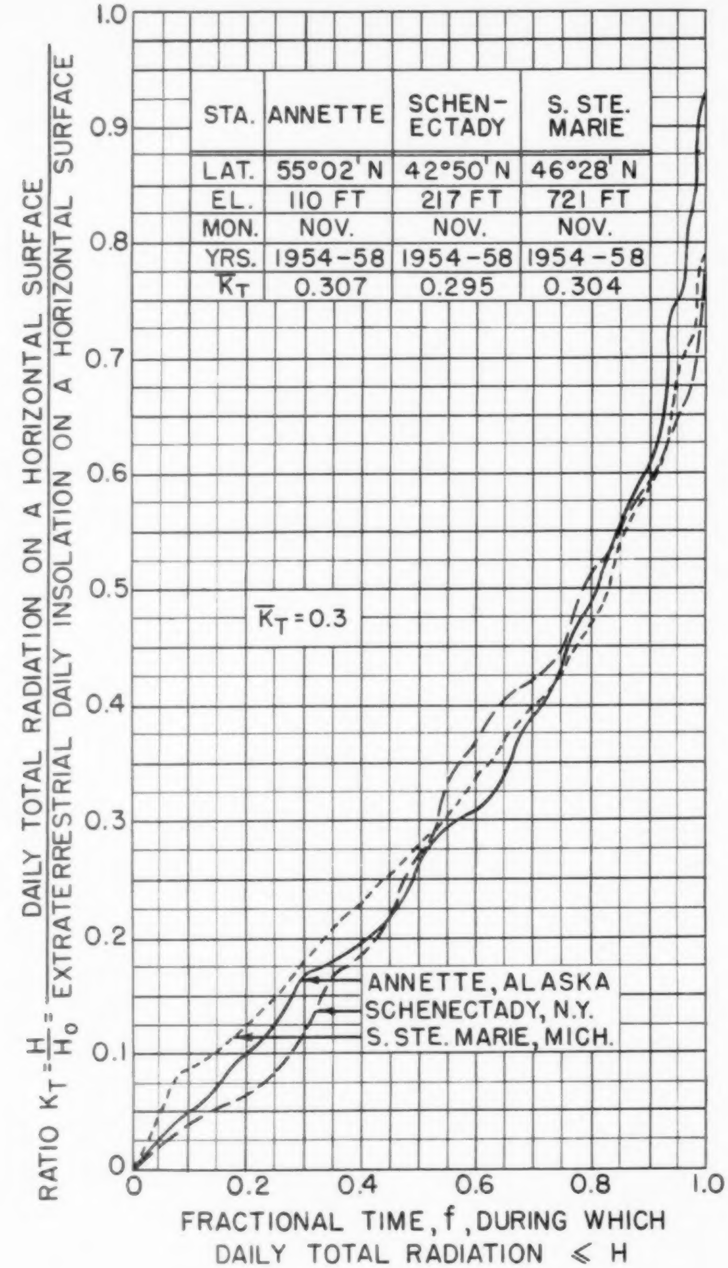

FIG. 9—Monthly K_T curves for $\bar{K}_T = 0.3$.

fuse radiation, $\bar{D}$. However, in order to compute $\bar{D}$, with the use of the relationship of Fig. 7, the statistical distribution of the daily total radiation must be known.

For reasons to be discussed it has been suspected that a correlation possibly exists among the statistical distribution curves of different localities. To test whether this indeed is the case, statistical distribution curves of daily total radiation for widely separated localities have been constructed and compared. Typical examples of these comparisons are shown in Figs. 9, 10 and 11.

Each of the curves of Fig. 9, 10 and 11 have been constructed using five year (primarily 1954–1958) data of daily total radiation from the Weather Bureau publication, Climatological Data, National Summary, and the curves have been so arranged that the values of $\bar{K}_T$ for curves on the same graph are approximately equal where

$$\bar{K}_T = \bar{H}/H_o \qquad [9]$$

and $\bar{H}$, the monthly average of the daily total radiation for the particular month at the particular locality under consideration, and H_o, the extraterrestrial daily insolation, have been obtained from Fig. 6. The statistical distribution curves so obtained will be termed the "monthly K_T curves" since they represent the statistical distribution of the quantity K_T and are constructed on a monthly basis.

A comparison of the different curves in the same figure shows that although the curves are not identical, the differences among them are not large and may be neglected for many practical purposes. The fact that such widely separated localities as Schenectady, New York, and Annette, Alaska, in Fig. 9 and localities with as much difference in elevation as Albuquerque, New Mexico, and Wake Island in Fig. 11 should have almost identical monthly K_T curves indicates that such a

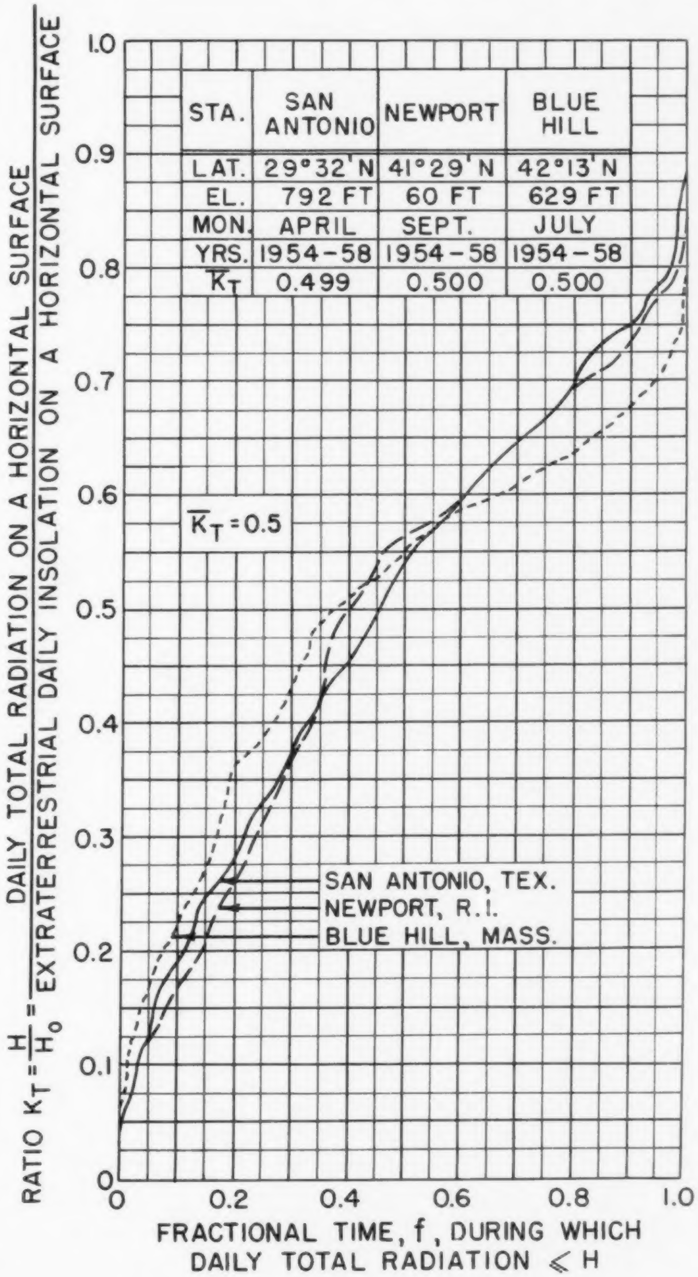

FIG. 10—Monthly K_T curves for $\bar{K}_T = 0.5$.

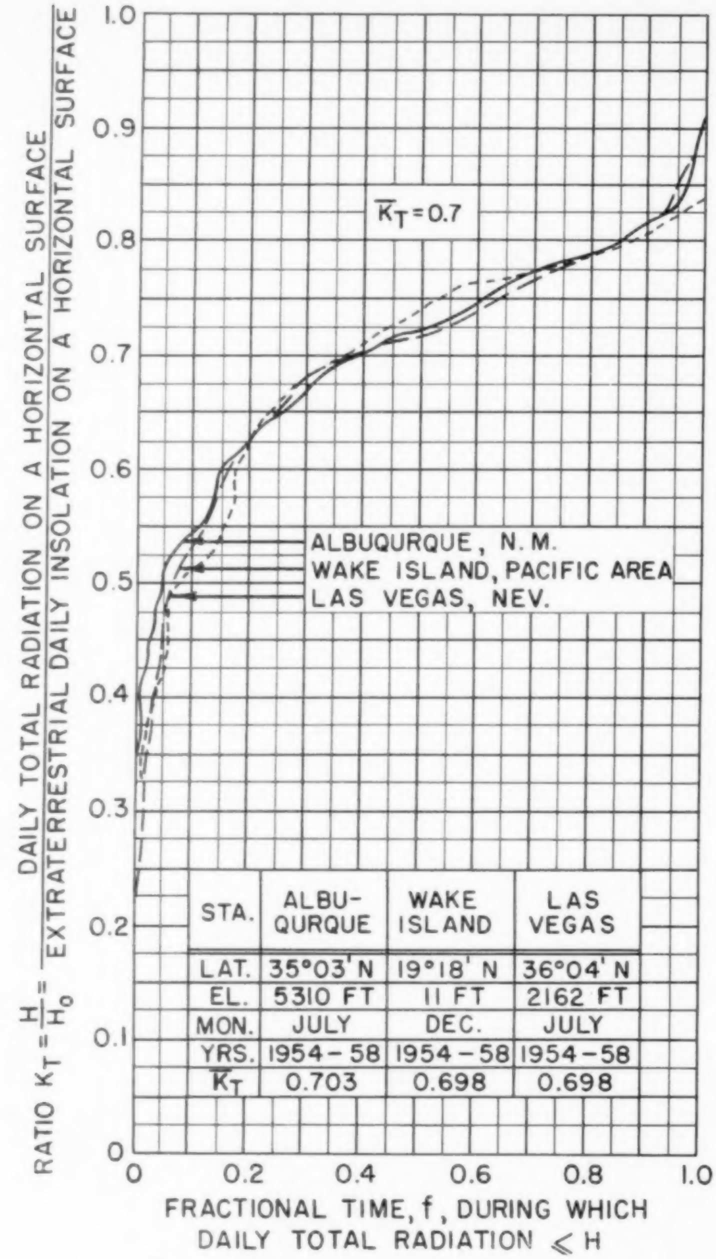

FIG. 11—Monthly K_T curves for $\bar{K}_T = 0.7$.

correlation between the forms of the monthly K_T curves and the values of $\bar{K}_T$ need not be restricted to these localities. Thus if a set of monthly K_T curves corresponding to different mean values of $\bar{K}_T$ is obtained, they may be used as a close approximation to the actual monthly K_T curves and can be utilized to determine the statistical distribution of the daily total radiation when the monthly average daily total radiation is known. A set of such "generalized monthly K_T curves" corresponding to $\bar{K}_T$ of 0.3, 0.4, 0.5, 0.6 and 0.7 has been obtained from the monthly K_T curves constructed with the data of the localities shown in Table 2. These generalized curves are shown in Fig. 12 and Table 3.

Relationship Between Monthly Average Daily Total and Monthly Average Daily Diffuse Radiation

The generalized monthly K_T curves of the preceding section may be used in conjunction with the curve in Fig. 7 to compute the monthly average of the daily diffuse radiation as follows.

Table 2.—Stations Selected for the Construction of the Generalized Monthly K_T Curves

Station	Latitude (North)	Elevation (ft.)	Month	$\bar{H}$ (ly/day)	$\bar{K}_T$	Period of Data
Annette, Alaska	55°02′	110	Nov.	199	.307	1954–1958
Schenectady, N. Y.	42°50′	217	Nov.	380	.295	1954–1958
S. Ste. Marie, Mich.	46°28′	721	Nov.	326	.304	1954–1958
Boston, Mass.	42°22′	15	Dec.	298	.399	1955–1958
Cleveland, O.	41°30′	787	Dec.	310	.400	1955–1958
Indianapolis, Ind.	39°44′	793	Nov.	434	.401	1954–1958
Oak Ridge, Tenn.	36°01′	905	Jan.	429	.399	1952, '54, '55, '57 '58
Put-in-Bay, O.	41°39′	575	Nov.	404	.396	1950–1953
State-College, Pa.	40°48′	1175	Jan.	357	.406	1954–1958
Atlanta, Ga.	33°39′	975	Jan.	468	.498	1954–1958
Blue Hill, Mass.	42°13′	629	July	994	.500	1954–1958
Newport, R. I.	41°29′	60	Sept.	730	.500	1954–1958
Ottawa, Ont.	45°20′		Apr.	815	.498	1954–1958
San Antonio, Tex.	29°32′	792	Apr.	902	.499	1954–1958
Seattle, Wash.	47°36′	14	Aug.	858	.502	1951, '52, '54, '55, '58
Apalachicola, Fla.	29°44′	13	Mar.	778	.600	1952, 1955–1958
Bismarck, N. D.	46°46′	1650	Aug.	862	.599	1954–1958
Cleveland, O.	41°30′	787	May	963	.597	1951, 1955–1958
Grand Lake, Colo.	40°15′	8389	Apr.	850	.598	1950–1953, 1957
Midland, Tex.	32°01′	2854	Oct.	661	.601	1954–1958
Rapid City, S. D.	44°09′	3165	Apr.	825	.600	1954–1958
Albuquerque, N. M.	35°03′	5310	July	997	.703	1954–1958
Grand Junction, Colo.	39°06′	4849	June	1019	.699	1954, '55, '57, '58
Las Vegas, Nev.	36°04′	2162	July	998	.698	1954–1958
Riverside, Calif.	33°58′	1050	Sept.	797	.700	1954–1958
Santa Maria, Calif.	34°56′	238	July	997	.700	1954–1958
Wake Islands, P.A.	19°18′	11	Dec.	635	.698	1954–1958

Table 3—The Generalized Monthly K_T Curves

K_T	Value of f for $\bar{K}_T$ = .3	.4	.5	.6	.7
.04	.073	.015	.001	.000	.000
.08	.162	.070	.023	.008	.000
.12	.245	.129	.045	.021	.007
.16	.299	.190	.082	.039	.007
.20	.395	.249	.121	.053	.007
.24	.496	.298	.160	.076	.007
.28	.513	.346	.194	.101	.013
.32	.579	.379	.234	.126	.013
.36	.628	.438	.277	.152	.027
.40	.687	.493	.323	.191	.034
.44	.748	.545	.358	.235	.047
.48	.793	.601	.400	.269	.054
.52	.824	.654	.460	.310	.081
.56	.861	.719	.509	.360	.128
.60	.904	.760	.614	.410	.161
.64	.936	.827	.703	.467	.228
.68	.953	.888	.792	.538	.295
.72	.967	.931	.873	.648	.517
.76	.979	.967	.945	.758	.678
.80	.986	.981	.980	.884	.859
.84	.993	.997	.993	.945	.940
.88	.995	.999	1.000	.985	.980
.92	.998	.999		.996	1.000
.96	.998	1.000		.999	
1.00	1.000			1.000	

It should be observed that the area under any monthly K_T curve is numerically the same as the value of $\bar{K}_T$, since from the definitions of $\bar{K}_T$ and "f" in Figs. 9, 10, 11 or 12,

$$\bar{K}_T = \bar{H}/H_0 = \frac{1}{H_0}\int_{f=0}^{f=1} H\,df = \int_{f=0}^{f=1} \frac{H}{H_0}\,df = \int_{f=0}^{f=1} K_T\,df \qquad [10]$$

However, since the ratio of D/H is a unique function of K_T as shown in Fig. 7, when $\bar{K}_d$ is defined as

$$\bar{K}_d = \bar{D}/H_o \qquad [11]$$

it is seen that

$$\bar{K}_d = \int_{f=0}^{f=1} \frac{D}{H_0}\,df = \int_{f=0}^{f=1} \frac{D}{H}\,K_T\,df \qquad [12]$$

Equation [12] states that when the ordinate, K_T, of a monthly K_T curve is multiplied by the ratio D/H from Fig. 7, the area under the curve so obtained is numerically equal to the value of $\bar{K}_d$. The value of $\bar{D}$ can then be obtained easily by multiplying $\bar{K}_d$ by the extraterrestrial daily insolation H_o from Fig. 6.

When the coordinates K_T of the generalized monthly K_T curves of Fig. 12 are multiplied by the ratio D/H from Fig. 7, the curves of Fig. 13 are obtained. The areas under these curves, according to Equation [12], are numerically equal to the values of $\bar{K}_d$. A graphical integration produces the result shown in Table 4.

The value of $\bar{K}_d$ corresponding to $\bar{K}_T$ = 0.75 in Table 4 is taken from Fig. 5, since a locality with $\bar{K}_T$ = 0.75 should have almost constant clear weather from

day to day and therefore K_d and K_T should remain almost constant from day to day and be respectively equal to $\bar{K}_d$ and $\bar{K}_T$.

It should be noticed that the results of Table 4, in which $\bar{K}_d$ is a single valued function of $\bar{K}_T$, can be obtained only when a correlation between the monthly K_T curves and $\bar{K}_T$ such as those shown in Figs. 9, 10 and 11 exists. Indeed this was the reason which initially led the authors to suspect such a correlation, since the relationship between K_d and K_T of Fig. 5, derived from the data of Blue Hill, strongly suggests the existence of a similar unique relationship between $\bar{K}_d$ and $\bar{K}_T$.

In examining Table 4, it should be noted that a locality may be considered to be extremely cloudy, if on a monthly average basis, the daily extraterrestrial solar radiation transmitted through the atmosphere is only 30% ($\bar{K}_T = 0.30$). However, a locality may be considered to be very sunny if $\bar{K}_T = 0.70$. The results of Table 4 show that irrespective of the markedly dif-

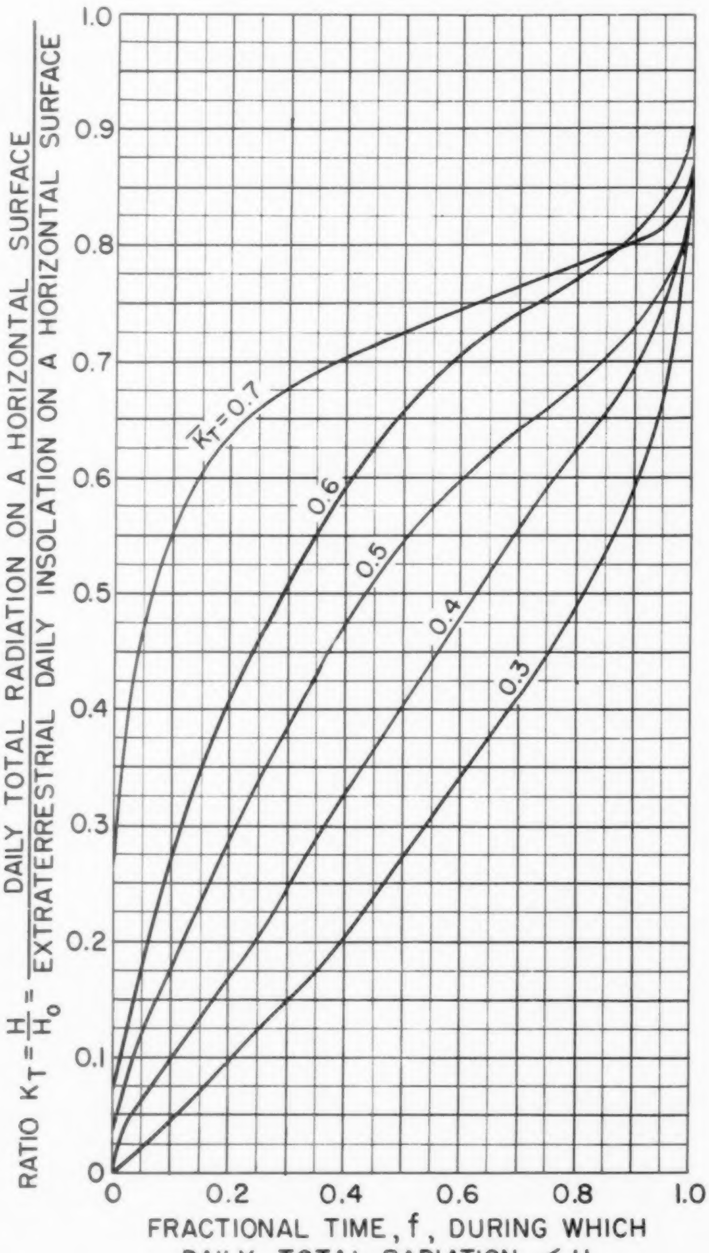

FIG. 12—The generalized monthly K_T curves.

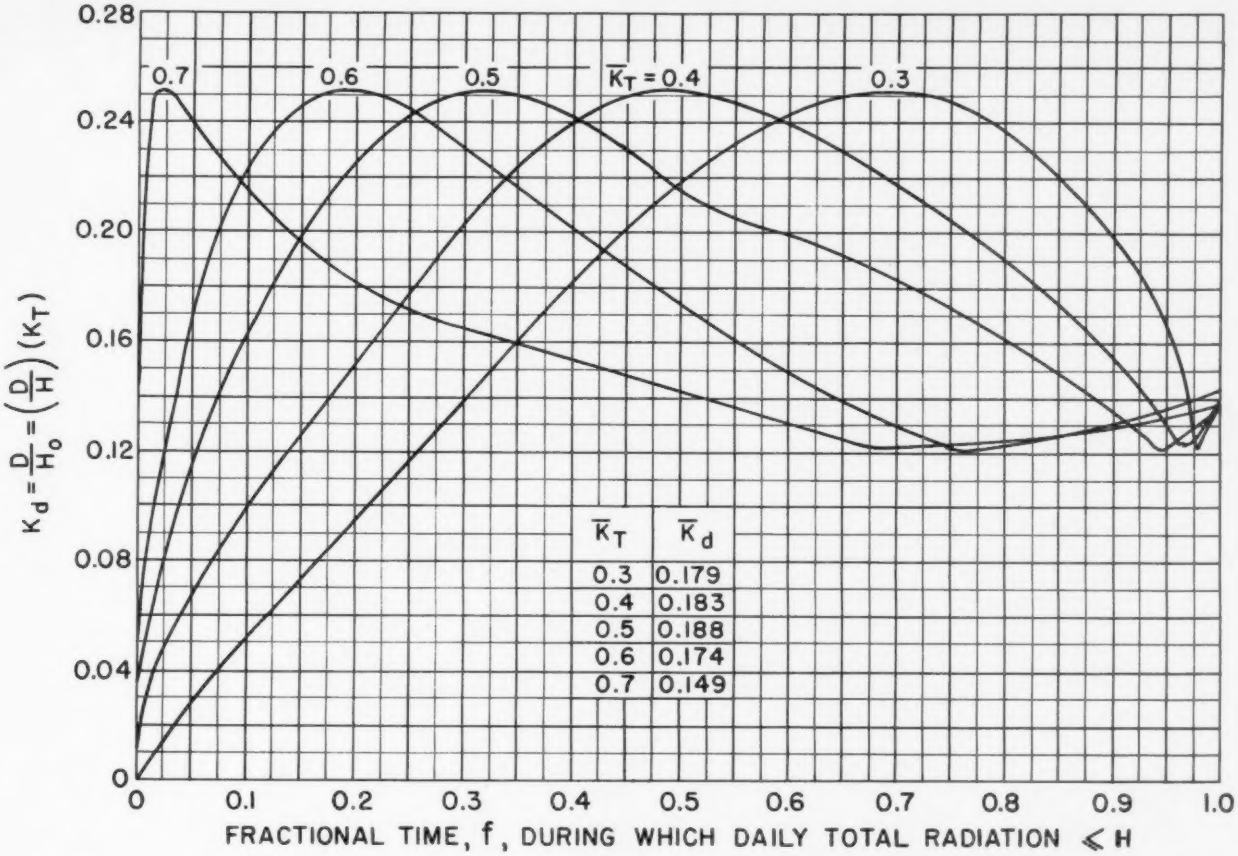

FIG. 13—Curves for the determination of $\bar{K}_d$.

TABLE 4—The Relation Between the Monthly Average Daily Total and the Monthly Average Daily Diffuse Radiation

$\bar{K}_T$	0.3	0.4	0.5	0.6	0.7	(0.75)
$\bar{K}_d$	0.179	0.183	0.188	0.174	0.149	(0.125)

ferent atmospheric conditions associated with the different values of $\bar{K}_T$, on a monthly average basis, the fractions of the extraterrestrial daily insolation transmitted through the atmosphere as diffuse radiation, i.e. the values of $\bar{K}_d$, show only a very moderate variation—from a minimum of 0.125 to a maximum of 0.188. Furthermore an analysis of the data of daily total radiation published by the U. S. Weather Bureau shows that for a great majority (over 70%) of localities and months, the values of $\bar{K}_T$ lie in the range of 0.3 to 0.6. Thus one should expect, from the results of Table 4 alone, that for many localities $\bar{K}_d$ is within the range from 0.174 to 0.188. From the limited diffuse radiation data available, the twelve months average of $\bar{K}_d$ is 0.178 at Blue Hill, Massachusetts, (10 year average);[8] 0.185 at Nice, France, (3 year average);[9] 0.189 at Helsingfors, Finland, (4 year average);[10] and 0.205 at London, England, (5 year average).[11] A further examination of the data of London shows that the reason that the experimental values of $\bar{K}_d$ are higher than those predicted is due, at least in part, to the fact that a "shading ring" correction of 1% to 6% had been added to the measured diffuse radiation. The agreement would have been entirely satisfactory if this correction had not been applied to the measured diffuse radiation as with the data of the other localities.

The ratio $\bar{D}/\bar{H}$ plotted as a function of $\bar{K}_T$ is shown in Fig. 14. The experimental ratio for each month and for each of the four localities are also shown on the same graph for comparison.

Relationship Between Hourly and Daily Diffuse Radiation

A knowledge of the average intensity of diffuse radiation at different times of the day is needed in many problems dealing with solar radiation. Since solar radiation data are not presented for intervals shorter than one hour, the nearest approach to the true average intensity at an instant obtainable from the solar radiation data commonly available is the hourly average intensity. Again it must be emphasized that extremely variable cloudiness precludes the possi-

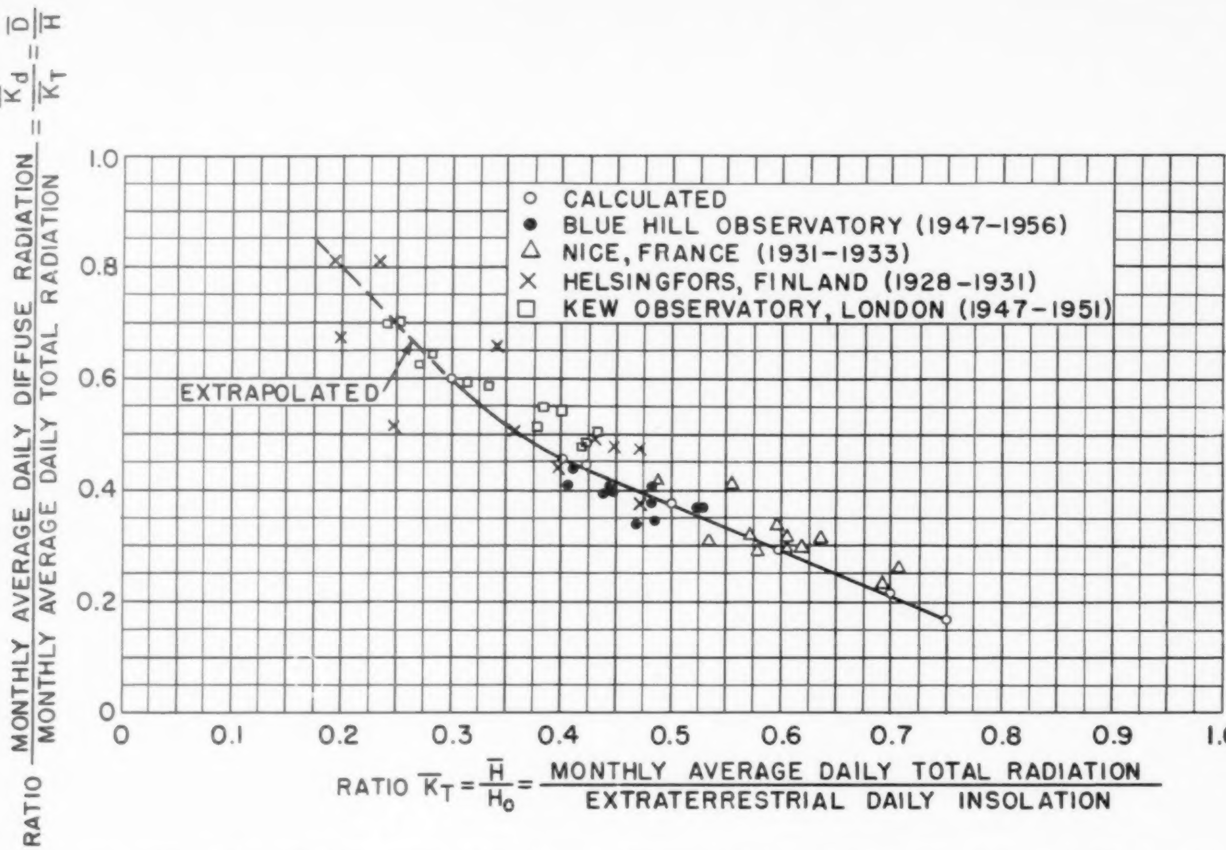

FIG. 14—The ratio of the monthly average daily diffuse radiation to the monthly average daily total radiation as a function of the cloudiness index $\bar{K}_T$.

bility of obtaining a true instantaneous radiation intensity during cloudy days except from direct experimentation.

By Equation [11]

$$\bar{D} = \bar{K}_d H_o \qquad [13]$$

If the assumption is made that the same fraction, $\bar{K}_d$, also represents the ratio of the average intensity of diffuse radiation to the extraterrestrial radiation intensity, i.e.

$$\bar{I}_{dh} = \bar{K}_d I_{oh} \qquad [14]$$

where $\bar{I}_{dh}$ is the average intensity of diffuse radiation received on a horizontal surface, then the ratio r_d of the average intensity of diffuse radiation to the daily diffuse radiation is

$$r_d = \bar{I}_{dh}/\bar{D} = I_{oh}/H_o \qquad [15]$$

The correctness of this assumption can be tested only when the ratio computed by means of Equation [15] is compared with the ratio derived from the experimental data.

An expression for H_o is given in Equation [5], and the instantaneous radiation intensity can be shown to be

$$I_{oh} = rI_{sc}(\cos L \cos \delta \cos \omega + \sin L \sin \delta) \qquad [16]$$

Therefore

$$r_d = \frac{\pi}{24} \frac{\cos L \cos \delta \cos \omega + \sin L \sin \delta}{\cos L \cos \delta \sin \omega_s + \omega_s \sin L \sin \delta} \qquad [17]$$

When the sunset hour angle, ω_s, of Equation [6], is substituted into Equation [17], the expression is obtained,*

$$r_d = \frac{\pi}{24} \frac{\cos \omega - \cos \omega_s}{\sin \omega_s - \omega_s \, \text{cps} \, \omega_s} \qquad [18]$$

Using the ten year data for Blue Hill, Massachusetts,[8] and the four year data for Helsingfors, Finland,[12] the experimental ratio of the monthly average hourly to daily diffuse radiation for the hours: 11:00–12:00 a.m. and 12:00–1:00 p.m., 10:00–11:00 a.m. and 1:00–2:00 p.m., etc., are plotted as shown in Fig. 15 against the sunset hour angle ω_s computed by means of Equation [6] with the use of the mean solar declination for each month. The data for the morning and afternoon hours symmetrical with respect to solar noon have been combined in obtaining these ratios. If these average

* An equation which is slightly different, but practically the same as Equation [18] was first derived by Whillier in his investigation of the relation between the hourly and daily total radiation on a horizontal surface to be discussed in the following section.

hourly diffuse radiation are considered as the average intensities of diffuse radiation at the mid-point of these hours, a comparison with the theoretical ratio r_d of Equation [18] can be made. The ratio r_d computed by means of Equation [18] using the hour angle at $\frac{1}{2}$, $1\frac{1}{2}$, $2\frac{1}{2}$, etc., hours from solar noon is shown plotted in Fig. 15 as the solid curves.

The excellent agreement between the experimental ratios and those computed by means of Equation [18] substantiates the assumption made in Equation [14]. Thus both Equation [14] and Fig. 15 may be utilized for the determination of the average intensity of diffuse radiation when the value of $\bar{K}_d$, which can be determined from Table 3 and Fig. 14, is known.

Relationship Between the Hourly and Daily Total Radiation

If the subscript "d" for diffuse radiation in Equations [13] and [14] is replaced by the subscript "T" for total radiation, an expression which is identical to r_d

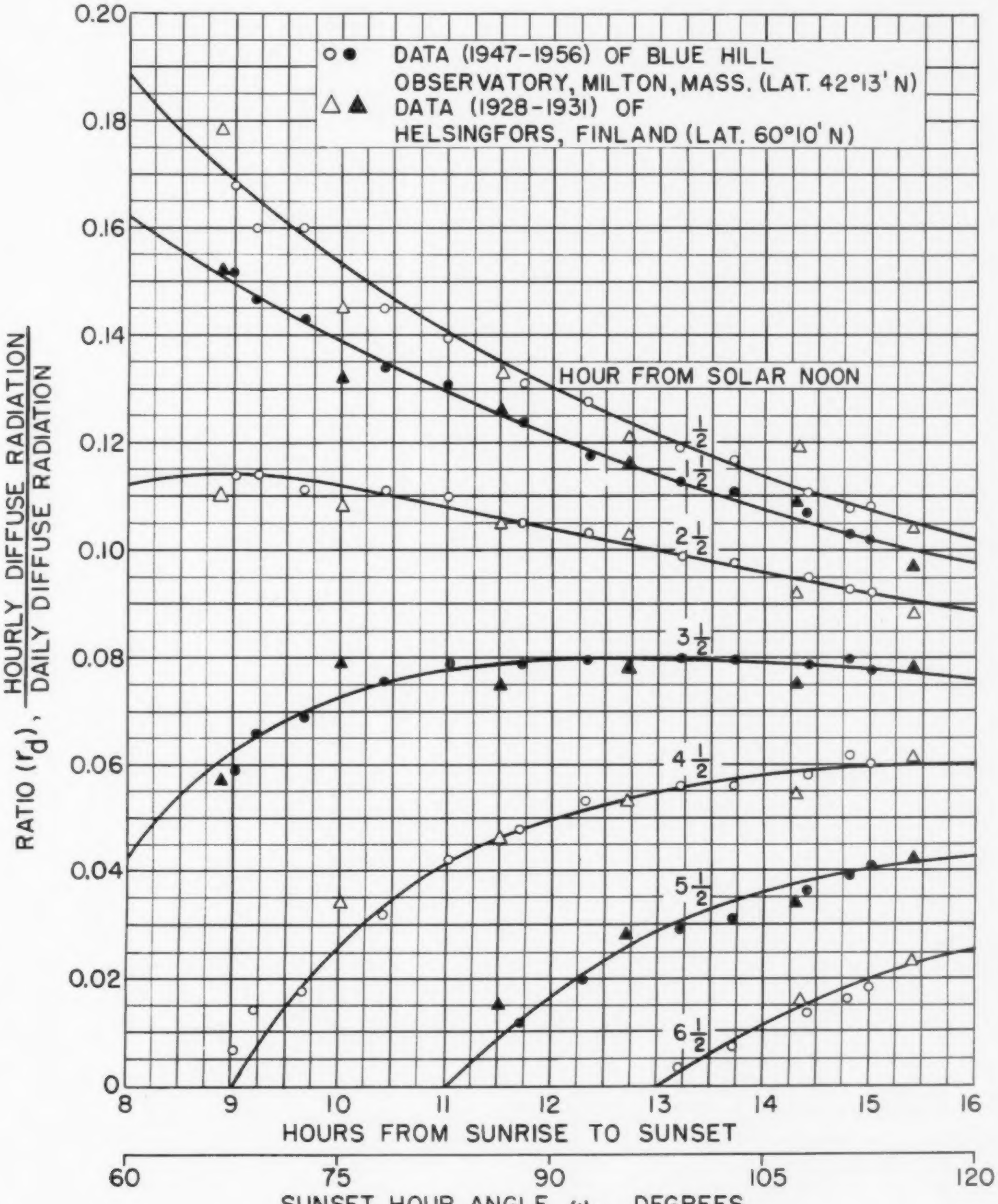

Fig. 15—Theoretical and experimental ratio of the hourly diffuse radiation to the daily diffuse radiation.

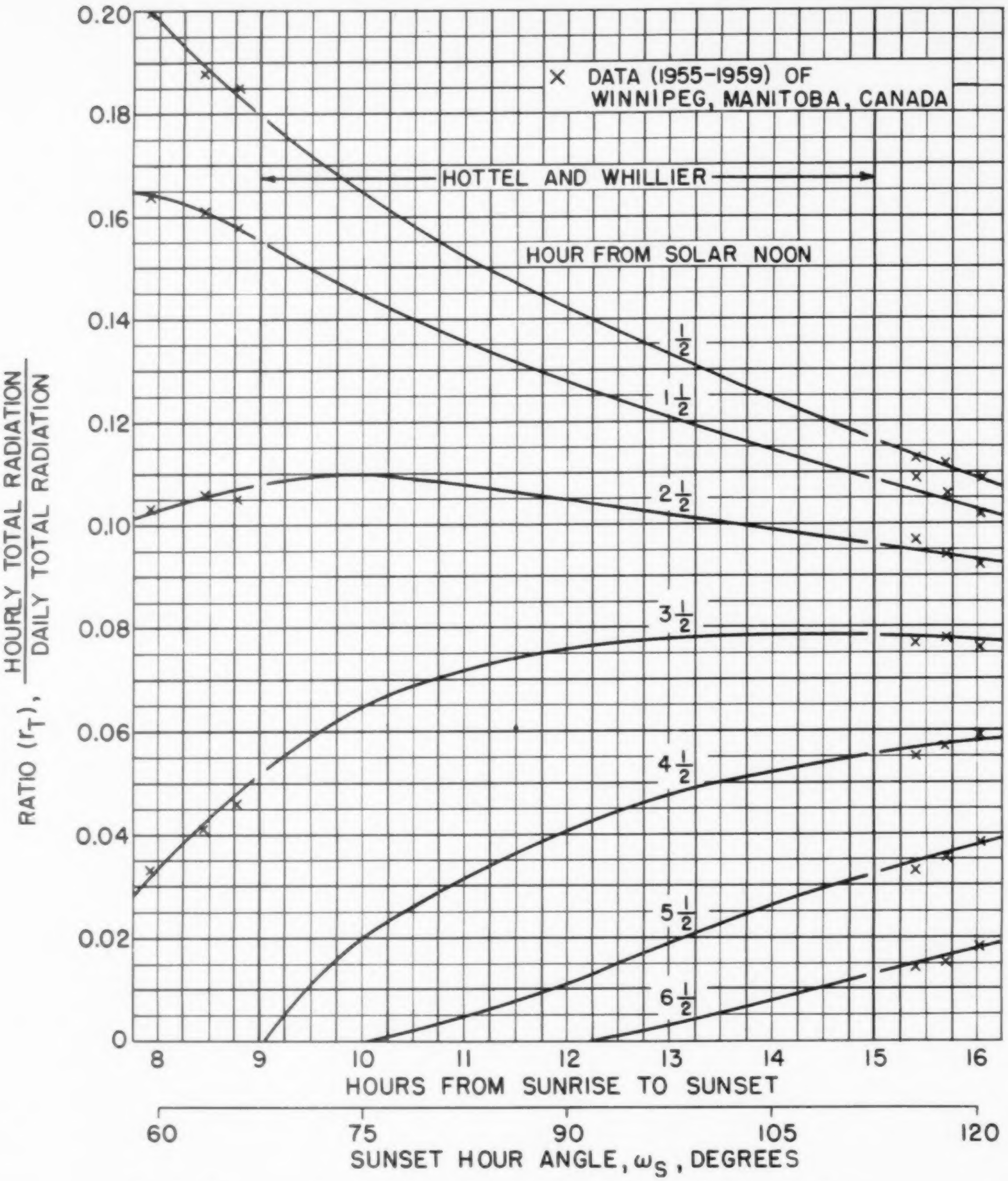

FIG. 16—Experimental ratio of the hourly total radiation to the daily total radiation.

of Equation [18], is obtained for r_T, the ratio of the average intensity of total radiation incident upon a horizontal surface to the daily total radiation received on the horizontal surface. It was shown by Whillier[13] and Hottel and Whillier[14] that the experimentally determined ratios r_T are different from those computed by means of Equation [18]. However, it was also shown that when the experimental ratios r_T derived from the data of widely separated localities are plotted against the sunset hour angle, a mean curve for each hour is obtained such that the deviation of any individual point from the mean curve is no more than ±5% for all hours between 9:00 a.m. and 3:00 p.m. sun time. The experimental curves in Fig. 16 in the range of 9 to 15 hours from sunrise to sunset are those presented by Hottel and Whillier.[14] The extension beyond this range has been made with data from Winnipeg, Canada.[15]

The following two examples illustrate some of the possible applications of the relations derived in the preceding sections.

Example 1: Estimate the intensities of diffuse and

total radiation on a horizontal surface at 12:00 noon on June 23 at a locality on 36°N latitude. The direct radiation intensity, I_{Dn}, at normal incidence, according to Threlkeld and Jordan,[16] is 280 Btu/hr-sq ft for the assumed basic atmosphere. The solar altitude is 77.5°.

Solution: From Table 1, on June 23, $r = 0.9670$. Therefore, $I_{on} = rI_{sc} = (0.9670)(442) = 428$ Btu/hr-sq ft and $\tau_D = I_{Dn}/I_{on} = 280/442 = 0.655$. By means of Equation [1], $\tau_d = 0.2710 - (0.2939)(0.655) = 0.079$. Thus $I_{dh} = \tau_d I_{oh} = (0.079)(428)(\sin 77.5°) = 33$ Btu/hr-sq ft and $I_{Th} = I_{Dh} + I_{dh} = (280)(\sin 77.5°) + 33 = 307$ Btu/hr-sq ft.

Had the intensity of total radiation of 307 Btu/hr-sq ft been given, I_{dh} and I_{Dn} can be computed as follows: Since $\tau_T = I_{Th}/I_{oh} = 307/(428)(\sin 77.5°) = 0.734$, and by means of Equation [2] $\tau_d = 0.3840 - (0.4160)(0.734) = 0.079$, $I_{dh} = \tau_d I_{oh} = 33$ Btu/hr-sq ft as before. Therefore, $I_{Dn} = (I_{Th} - I_{dh})/\sin \alpha = (307 - 33)/\sin 77.5° = 280$ Btu/hr-sq ft.

Example 2: The five year (1954–1958) average of the daily total radiation, $\bar{H}$, on a horizontal surface for January in Indianapolis, Indiana, (Lat. 39°44′), is 553 Btu/day-sq ft according to data published by the U. S. Weather Bureau in Climatological Data, National Summary. The average of the daily diffuse radiation and the average intensities of total and diffuse radiation during the hour 11:00–12:00 and 12:00–1:00 are to be estimated.

Solution: By means of Fig. 6 or Equation [5] $H_o = 1370$ Btu/day-sq ft. Therefore $\bar{K}_T = \bar{H}/H_o = 553/1370 = 0.403$, and by means of Fig. 14, $\bar{D}/\bar{H} = 0.454$. Hence $\bar{D} = (\bar{D}/\bar{H})(\bar{H}) = (0.454)(533) = 242$ Btu/day-sq ft.

Since the sunset hour angle, ω_s, is given by Equation [6], and on January 16, the declination is −21°, $\cos \omega_s = -(\tan 39°44′)(-\tan 21°) = 0.323$, $\omega_s = 71°$ (or $\frac{71}{15} \times 2 = 9.45$ hours between sunrise and sunset). From Figs. 16 and 15, $r_T = 0.172$ and $r_d = 0.161$. Therefore, the average intensities of total and diffuse radiation during the hours 11:00–12:00 and 12:00–1:00 are respectively, $\bar{I}_{Th} = r_T\bar{H} = (0.172)(553) = 95$ Btu/hr-sq ft and $\bar{I}_{dh} = r_d\bar{D} = (0.161)(242) = 39$ Btu/hr-sq ft.

Using the generalized monthly K_T curves of Fig. 12 or Table 3, it is possible to determine approximately, from the given value of $\bar{H}$, the fractional times during which the daily total radiation is less than or equal to certain values. For example, according to Table 3 or Fig. 12, when $K_T = 0.20$, $f = 0.249$. Thus for 25% of the time (or $7\frac{1}{2}$ days during the month), the daily total radiation is less than or equal to $K_T H_o = (0.20)(1370) = 274$ Btu/day-sq ft during January in Indianapolis. Similarly for 76% of the time (or 23 days in the month) the daily total radiation is less than or equal to $(0.60)(1370) = 820$ Btu/day-sq ft. The actual average (1954–1958) number of days in January with radiation below the above values are respectively $6\frac{1}{2}$ and 23 days in Indianapolis.

The generalized monthly K_T curves can also be utilized to determine approximately the statistical distribution of the daily total radiation for localities where only an estimate of the monthly average of the daily total radiation is known[17] since the only information needed is the value of $\bar{H}$.

REFERENCES

1. Parmelee, G. V., "Irradiation of Vertical and Horizontal Surfaces by Diffuse Solar Radiation from Cloudless Skies," *ASHVE Transaction* **60:** 341–358, 1954.
2. Johnson, F. S., "The Solar Constant," *Journal of Meteorology*, **11:** 431–439, December, 1954.
3. Drummond, A. J. and Greer, H. W.: "Fundamental Pyrheliometry," *The Sun at Work* **3**(2): 3–5, 11, June, 1958.
4. Klein, W. H., "Calculation of Solar Radiation and the Solar Heat Load on Man," *Journal of Meteorology*, **5:** 119–129, August, 1948.
5. Moore, A. F. and Abbot, L. H., "The Brightness of the Sky," *Smithsonian Miscellaneous Collection*, **71**(4): 1–36, February, 1920.
6. Fritz, S., "Solar Radiation During Cloudless Days," *Heating and Ventilating*, **46:** 69–74, January, 1949.
7. Hand, I. F., "Methods of Calculating Solar Radiation Values at Blue Hill Observatory, Milton, Massachusetts," *Monthly Weather Review*, **82:** 43–49, February, 1954.
8. Diffuse and total radiation data for Blue Hill, Massachusetts, were obtained from Mr. C. V. Cuniff, U. S. Weather Bureau, Blue Hill Observatory, Milton, Massachusetts. For instrumentation and methods of measurement see: Hand, I. F. and Wollaston, F. A., "Measurements of Diffuse Solar Radiation at Blue Hill Observatory," *Technical Paper No. 18*, U. S. Department of Commerce, Weather Bureau, Washington, D. C., May, 1952.
9. Gorcynski, W., "Enregistrements due Rayonnement Solaire au Moyan des Solarigraphy et des Pyrheliographes," *Nice. Office Meteorologique, Annales*, Tome **11:** 117–165, 1933.
10. Lunelund, H., "Contribution to the Knowledge of Solar Radiation in Finland," *Finska Vetenskaps-Societeten, Helsingfors, Commentationes Physico-Mathematicae*, **7**(11): 1–58, February, 1934.
11. Blackwell, M. J., "Five Years Continuous Recording of Total and Diffuse Radiation at Kew Observatory," *Paper of the Meteorological Research Committee (London)*, No. 895, 1954.
12. Lunelund, H., "Records of Solar Radiation in Helsingfors," *Finska Vetenskaps-Societeten, Helsingfors, Commentationes Physico-Mathematicae* **7**(1): 1–28, 1933.
13. Whillier, A., "The Determination of Hourly Values of Total Solar Radiation from Daily Summations," *Archiv fur Meteorologie, Geophysik und Bioklimatologie*, Vienna, Series B., **7:** 197–244, 1956.
14. Hottel, H. C. and Whillier, A., "Evaluation of Flat-Plate Solar Collector Performance," *Transaction of the Conference on the Use of Solar Energy*: The Scientific Basis, Vol. II, Part I, Section A, pp. 74–104, 1955.
15. Data of total radiation for Winnipeg, Canada, are obtained from Mr. D. M. Robertson, Regional Meteorologist, District Aviation Forecast Office, Winnipeg, Canada.
16. Threlkeld, J. L. and Jordan, R. C., "Direct Solar Radiation Available on Clear Days," *Heating, Piping and Air Conditioning*, **29:**(12): 135–145, December, 1957.
17. Fritz, S. and MacDonald, T. H., "Average Solar Radiation in the United States," *Heating and Ventilating*, **46**(7): 61–64, July, 1949.

Determination of the Temperature Dependence of Material Properties in Image Furnaces

By Tibor S. Laszlo and Murray S. Klamkin

Avco Research and Advanced Development, Wilmington, Massachusetts

A special testing method is described which makes it possible to determine a property of a specimen for narrow temperature intervals from measurements in the wide-range temperature distribution of an image furnace. The determination is based on the measurement of the property at several different flux levels of known temperature distribution.

INTRODUCTION

A serious limitation imposed by the fundamental optics of image furnaces is the non-uniformity of the flux across the image area. Due to the ratio of radiation source diameter and its distance from the image furnace, the recreated image has a more or less regular, bell-shaped flux distribution. Accordingly, a sample heated in an image furnace will have a similar temperature distribution. A single measurement of a property, e.g., electrical resistivity, of such a sample yields a value which cannot be related to any one temperature and is therefore meaningless.

A new experimental technique has been developed which makes it possible to obtain meaningful values of a property for narrow temperature intervals from measurements in the wide-range temperature distribution of an image furnace if the distribution is well defined. Such is the case in the solar furnace.

THE DETERMINATION OF PROPERTIES FOR A NARROW TEMPERATURE RANGE

In direct measurements of radiation properties it is only possible to obtain one effective value for the entire temperature range of the solar image. This range may reach from the ambient temperature at the periphery to 3000–3500°C at the center of the image. Thus, the directly measured value of any property (e.g. electrical resistivity, thermal expansion, etc.) has little, if any definitive meaning. If, however, the same measurement is also performed at a different temperature level, information may be obtained on the temperature dependence of the measured property.

By varying the position of the flux attenuator it is possible to obtain different temperature distributions in a sample. The different temperature distributions are illustrated in Fig. 1, as functions of the solar image diameter; $2L$ is the diameter of the image. Let this family of curves be represented by

$$T = \Phi(x, \lambda) \qquad [1]$$

where x is the distance from the edge of the image and λ the temperature distribution parameter.

The measured property per unit length at temperature T is denoted by $R(T)$. The value of the property of the sample for a given temperature distribution is

$$\bar{R} = 2\int_0^L R(T)\, dx \qquad [2]$$

or

$$\bar{R} = 2\int_0^L R\{\Phi(x, \lambda)\}\, dx \qquad [3]$$

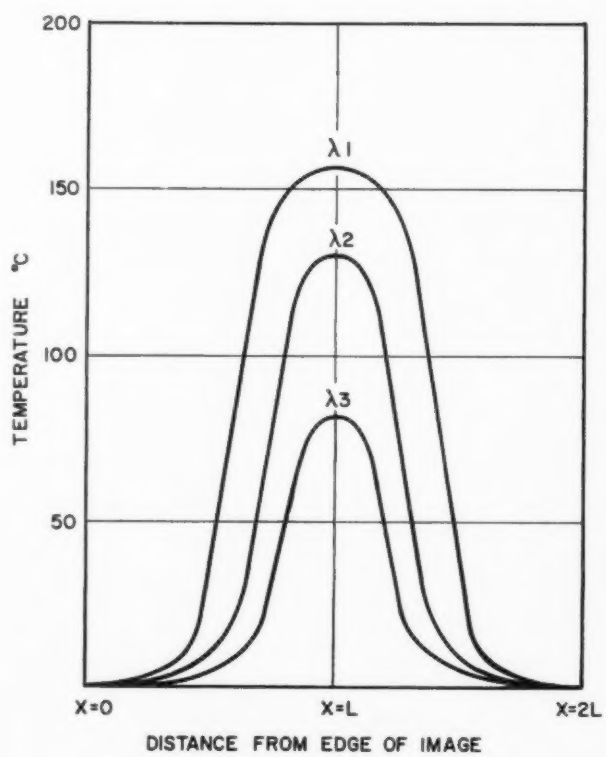

Fig. 1—IMAGE TEMPERATURE DISTRIBUTION

This is an integral equation relating the desired function $R(T)$ to the temperature distribution $\Phi(x, \lambda)$ and the measured value of the property $\bar{R}(\lambda)$. Since the function $\Phi(x, \lambda)$ is determined graphically, a numerical method of solution for $R(T)$ is proposed.

If it is desired to determine $R(T)$ for intervals of 300°C, at least ten values are needed to cover the entire temperature range of 3000°C. This necessitates the measurement of ten $\bar{R}(\lambda)$ values, one for each 300°C interval between the temperature maxima. Ten temperature distribution curves which depict $T = \Phi(x, \lambda)$ for the same intervals are also required. If $R(T)$ changes rapidly with temperature, the intervals may be decreased and the number of measurements increased in order to improve the accuracy of the method.

On the temperature distribution curves, horizontal lines are drawn corresponding to the specified temperature brackets, e.g., at $T_1 = 600°C$, $T_2 = 900° \cdots T_{10} = 3{,}300°$. The intersection of each line with each $\Phi(x, \lambda)$ curve determines a set of x and λ values. It then follows that the integral [3] can be approximated

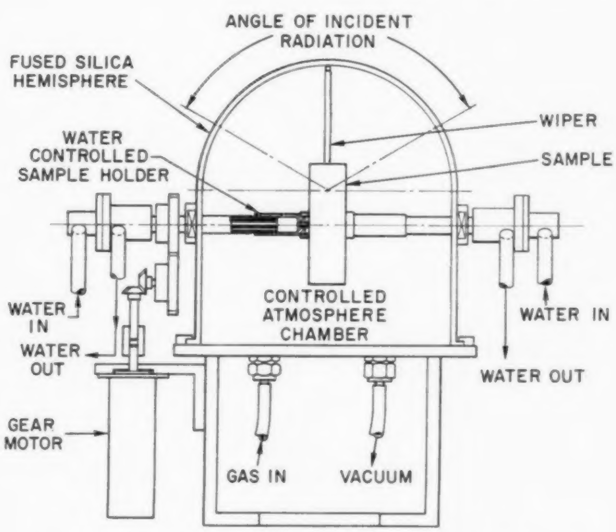

Fig. 2—CONTROLLED ATMOSPHERE ROTATING SAMPLE HOLDER

by the finite sum

$$\tfrac{1}{2}\bar{R}(\lambda) = R(\bar{T}_1)(x_1 - x_0) + R(\bar{T}_2)(x_2 - x_1) + \cdots R(\bar{T}_{10})(x_{10} - x_9) \qquad [4]$$

or

$$\bar{R}(\lambda) = 2\sum_{i=1}^{10} R(\bar{T}_1)(x_i - x_{i-1}) \qquad [5]$$

Where $2\bar{T}_1 = T_i + T_{i-1}$, $x_0 = 0$ and T_{10} is the maximum temperature obtained during the measurements. Consequently $x_{10} = L$.

From the ten equations, like [5], obtained for the ten different λ's, it is possible to determine the ten unknown $R(\bar{T}_i)$ values. The values obtained for $R(T)$ are plotted versus T, and a smooth curve is drawn from which values of R can be read off for each temperature interval, in this case intervals of 300°C.

In carrying out this experiment it is important to determine accurately the temperature distribution of the sample placed in the image area as called for in Fig. 1. This is done with a specially designed radiometer.[1] Not only is it necessary to control the maximum temperature at the center but also the temperature at the coolest part of the sample.

A sample holder has been designed for employment with this method (Fig. 2). The end plates of the sample holder are water cooled in order to keep the temperature of the sample constant at the contact point. The sample can be rotated to maintain a uniform temperature around its circumference. A very thin rod-shaped sample is used, and, accordingly, the only temperature variation occurs along its length.

ACKNOWLEDGMENT

The research reported in this paper has been sponsored by the Air Force Cambridge Research Laboratories, Air Force Research Division (ARDC) under contract AF19(604)-7204.

REFERENCE

1. T. S. Laszlo. "Temperature and Flux versus Geometrical Perfection". *Solar Energy*, **1**(2–3): 1957. p. 78

Recommendations and Suggested Techniques for the Manufacture of Inexpensive Solar Cookers

James R. Jenness, Jr.

HRB-Singer, Inc. State College, Pennsylvania

Solar cookers of the focusing-reflector type have been considered too expensive for use in the arid non-industrial regions which need them most. However, it should be possible to fabricate reflectors from cheap materials by hand-craft techniques, making possible their manufacture at low cost in small dispersed cottage industries. Solar cooking efficiency could be improved by the use of a cooking pot with a selective-black bottom surface and convection-shielding skirt. With such a cooking pot, specifically designed for use with a solar reflector, adequate cooking power could be obtained with a reflector of poor optical quality.

INTRODUCTION

Solar energy is available free to the consumer but in most cases requires a substantial investment in capital equipment to make possible its conversion to usable form. It is most easily converted to heat, and cooking is an application which can make use of it in this form. A family-sized solar cooker would be a useful piece of equipment in areas where sunshine is abundant and fuel is scarce, but unfortunately, presently-available solar cookers require an initial investment beyond the resources of most natives of these areas.

HRB-Singer has developed techniques for the fabrication of paraboloids by centrifugal casting.[1] Precision laminated paraboloidal microwave antennas up to 4 feet in diameter have been made from centrifugally-formed molds. In an experiment, one of these 4-foot-diameter reflectors was covered with 3″ x 18″ strips of aluminum foil, improvising a solar radiation collector which delivered approximately 100 watts to water in a can suspended at its focus. In view of this result, it is of interest to consider the possibility of developing techniques by which native craftsmen might be able to manufacture paraboloidal solar reflectors from cheap materials at a cost within the reach of the people of non-industrial regions. Increases in solar cooking efficiency which can be achieved by improvements in the design of the cooking pot used with the reflector make it possible to obtain useful cooking power with an easily-fabricated reflector.

SOLAR COOKER PRINCIPLES

Solar cookers of various types have been devised, but for present purposes interest will be restricted to the type which broils, fries, or boils food at the focus of a concave radiation-collecting reflector. The performance of such a cooker is described by the equation

$$W = St\,RA\alpha - a\,\epsilon\,\sigma T^4 - q$$

where

- W is the power applied to cooking,
- S is the solar constant, 1350 watts per square meter falling on the earth,
- t is the atmospheric transmission factor or the portion of this solar power reaching the earth's surface,
- R is the portion of incident radiation reflected by the collector and focused on the food container,
- A is the profile area of this collecting reflector,
- α is the portion of collected radiation absorbed by the food container,
- a is the area of the outer surface of this container,
- ϵ is the infrared emissivity of its outer surface,
- σ is the Stefan-Boltzmann radiation constant, 5.672 (10^{-8}) watt per square meter per (degree Kelvin)^4.
- T is the absolute temperature at the food container's outer surface.

and

- q is the rate of heat loss from the food container by convection.

The quantity most directly under the designer's control is A, but W can also be increased by maximizing R and α and minimizing ϵ and q. Efficiency is also increased by minimizing a, but it must remain large enough to insure interception of all convergent rays from the reflector. In general, it is preferable to use a cooking pot of convenient size, increasing A if necessary to compensate for the area of the reflector shaded by the pot. If the food container is of metal, T is very nearly the same as the temperature of the food and depends on the cooking method.

Boiling is a cooking method of particular interest, and for this application T is 100 degrees Centigrade (373 degrees Kelvin). If $t = 50\%$, $R = 80\%$, $A = 1$ square meter, $\alpha = 90\%$, $a = 0.1$ square meter, and $\epsilon = 90\%$, the net amount of the first two terms in the equation is 293 watts. On a calm or moderately windy day q should be less than 100 watts if the cooker is in a sheltered location, so W should be 200 watts under ordinary conditions. It is apparent that a substantial saving in fuel will result if the solar device is used for a significant portion of a family's cooking. Also, the labor involved in the care and operation of such a device is much less than that required for fuel gathering.

The reflector is the most expensive component of such a solar cooker, so our primary objective is the reduction of reflector manufacturing costs. One factor contributing to the expense of presently-available solar cookers is the emphasis given to light weight, collapsibility, and neat appearance. A serviceable reflector shell could probably be manufactured from cheap materials by native craftsmen at a fraction of the cost of present models. The major cause of high reflector cost is the expense of surfacing by polishing, anodizing, evaporation-coating, electroplating, and other techniques requiring special skills and equipment. A surface of adequate reflectivity can be produced by covering the reflector's concave surface with aluminum foil. Damage to such a surface can be easily repaired by pasting on patches of foil, and if necessary, the entire reflector can be resurfaced at low cost.

REFLECTOR FABRICATION TECHNIQUES

The only special equipment required for the fabrication of a reflector shell is a convex paraboloidal die shown in Figure 1a. The surface of this die is first coated with wax or grease, then a layer of wood pulp, papier mâché, or laminated newspaper is spread over it as shown in cross section in Figure 1b. A paper laminate can be made by dipping pieces of newspaper in dilute flour paste ($\frac{1}{2}$ to $\frac{1}{10}$ the concentration normally used with wallpaper) then spreading them over the die. After a few layers are built up, they are pressed to squeeze out excess liquid and make them conform to the paraboloidal surface. This process is repeated until the compressed laminate is $\frac{1}{8}$ to $\frac{1}{4}$ inch thick, then the rim of a wooden "wagon wheel" reinforcing framework is glued in place as shown in cross section in Figure 1c.

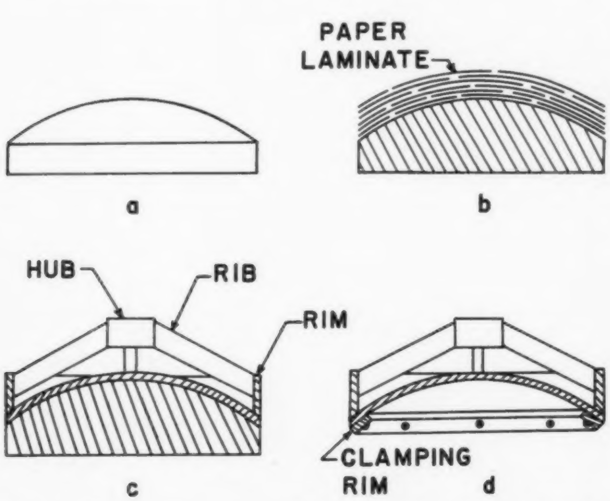

FIG. 1—Schematic of the Reflector Fabrication Method. (a) Convex Paraboloidal Die, (b) Paper Laminate Spread Over its Surface, (c) Reinforcing Framework Attached, (d) Cross Section of Finished Reflector.

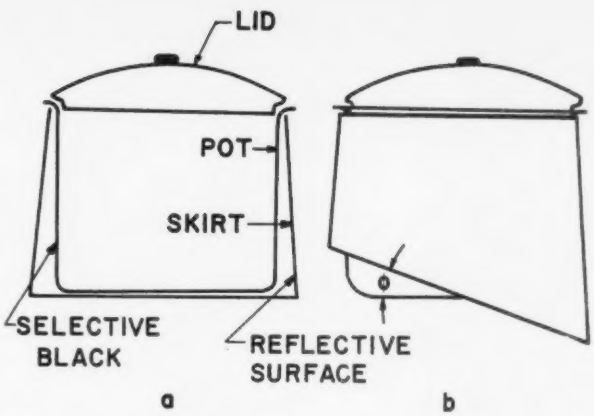

FIG. 2—Cooking Pots for Use with a Solar Reflector. (a) In the Tropics (Cross Section), (b) At Higher Latitudes.

When the laminate and glue have dried, the shell is removed from the die, and strips of aluminum foil are pasted onto its surface. Strips 2 to 3 inches wide can be applied to give a surface with very few wrinkles or overlaps. Finally, a front rim is fastened on as shown in Figure 1d. If this clamping rim is a stiff hoop, and if the shell is in contact with the reinforcing framework only at its periphery, the warping and buckling to which such a paper laminate is susceptible should be manifested only as a slight variation in the reflector's focal length.

This operation should be accomplished by 6 to 8 man-hours of effort. Perhaps the native craftsman can adapt the fabrication technique to his own particular situation, taking advantage of cheap materials available locally. (Woven basketry might be used in place of the "wagon wheel" reflector backing if sufficiently stiff clamping rims can be obtained.) Thus, the unit material cost might approach 25¢, the approximate cost of aluminum foil to surface a reflector. Convex wire-reinforced plaster paraboloidal dies could probably be cast from a centrifugally-formed master concave paraboloidal mold at a unit cost of $10.00 or less, so a small reflector-fabricating shop could be set up with quite modest capital. Wide distribution of these convex

tools could provide the basis for a dispersed cottage industry.

Improved Cooking Pot Design

Such a solar reflector would be more effective if it were used in conjunction with a cooking pot specifically designed for this application. In the calculation of cooking power above, it was assumed that α and ϵ were both 90%. If the bottom of the pot has a selective-black coating such as has been developed by Hottel and Unger[2] and by Kokoropoulos, Salam, and Daniels,[3] with $\alpha = 90\%$ and $\epsilon = 10\%$, cooking power obtained from the same reflector is increased 75%.

Convection losses can be reduced by skirts around the pot as shown in Figure 2. The simpler type (Figure 2a) could be used at mid-day in the tropics. In the early morning and later afternoon, and all day at higher latitudes, a slanted skirt as shown in Figure 2b is required. The slant angle ϕ is determined by the latitude, time of day, and focal-length-to-diameter ratio of the radiation-collecting reflector. The inside of the skirt should have a reflective surface so that rays not striking the pot directly will be reflected onto it. This will make the focusing adjustment less critical. Convection losses will of course be most easily reduced if the cooker is set up near a wall or other windbreak.

It appears reasonable to assume that such a cooking pot could reduce convection and re-radiation losses by 90%. Then cooking power of 466 watts could be attained under the conditions assumed in the first calculation. It is of considerable interest to note that 100 watts could be delivered to the contents of such a pot if the parameter R in the equation is only 21%. Thus, a quite crude reflector would be an adequate heat collector for such a pot.

Kokoropoulos, Salam, and Daniels[3] have indicated that it is easiest to apply durable selective-black coatings to small objects intended to operate at temperatures not much above 100°C. Therefore, it would seem that the manufacture of solar cooking pots, rather than large flat industrial heat collectors, offers the greatest opportunity for early utilization of such coatings.

CONCLUSIONS

Improved cooking pot design, rather than further refinements in reflector construction, offers the best opportunity for the advancement of solar cooking in non-industrial regions. With a selectively-absorbing convection-shielded pot, an easily-fabricated reflector can collect adequate solar cooking power. Moreover, small devices such as cooking pots lend themselves to large-scale manufacture and distribution more readily than large reflectors. Reflectors of sufficient radiation-collecting power can probably be manufactured near to those who would use them by craftsmen in dispersed cottage industries. A small reflector-fabricating shop could be established with a relatively small investment, a convex paraboloidal die being the main capital equipment required.

REFERENCES

1. Georg Hass and James R. Jenness, Jr., *Journal of the Optical Society of America*, **48:** 86–87 (February 1958).
2. H. C. Hottel and T. A. Unger, *Solar Energy*, **III-3:** 10–15 (October 1959).
3. Panos Kokoropoulos, Ehab Salam, and Farrington Daniels, *Solar Energy*, **III-4:** 19–23 (December 1959).

COMMENT ON SELECTIVE BLACK COATINGS

It is of interest to note that Hass, Schroeder and Turner[1] have developed surface coatings with very good selective absorption characteristics. These coatings are not used for solar heat collectors but for mirrors in infrared optical systems where it is desired to exclude visible light. They are applied by evaporation in vacuum, so they can not compete economically with coatings such as have been developed by Kokoropoulos, Salam and Daniels[2] and by Hottel and Unger.[3]

A selective black coating should be highly absorbing at wavelengths less than 2.5 microns and transparent at longer wavelengths. Such a coating applied over a reflective surface absorbs shorter wavelengths while preserving the high reflectivity (low emissivity) of the substrate at longer wavelengths. Kokoropoulos, Salam and Daniels[2] have noted that a selectively absorbing coating should be of a thickness equal to or greater than the short wavelengths to be absorbed and less than $\frac{1}{10}$ of the longer wavelengths for which low emissivity is desired. This has been given a simple explanation by Hass[4] who notes that a very thin coating over a reflective surface contains only the portion of the standing wave pattern near the node at the reflecting surface. A coating of half-wave or greater thickness contains regions of maximum amplitude in the standing wave pattern and thus has more energy available for absorption. Therefore, a thin coating of a uniformly absorbing material over a reflecting surface would absorb shorter wavelengths but not wavelengths large relative to the coating thickness. A coating material transparent to middle infrared wavelengths with high absorption in the solar spectrum and far-infrared is practically as good as a completely far-infrared-transparent, short-wavelength-absorbing coating.

REFERENCES

1. Georg Hass, H. H. Scroeder and A. F. Turner, *Journal of the Optical Society of America*, **46:** 31–35 (January 1956).
2. Panos Kokoropoulos, Ehab Salam and Farrington Daniels, *Solar Energy*, **III-4:** 19–23 (December 1959).
3. H. C. Hottel and T. A. Unger, *Solar Energy*, **III-3:** 10–15 (October 1959).
4. Georg Hass, *Journal of the Optical Society of America*, **45:** 945–952 (November 1955).

JAMES R. JENNESS, JR.
HRB-Singer, Inc.
State College, Penna.

Solar Abstracts

Prepared by Milton D. Lowenstein, Director, Technical Research Service Center

Abstracts, it may be observed, are useful to the extent that they are readily available at those critical moments in research and development activities when the advancement of a project depends upon objective and well recognized authority.

The Solar Energy Technical Research Service Center is establishing a source of information and a routine for supplying data as soon as they are received and processed. All the material in the library, correspondence on technical matters and research reports are being classified and arranged for quick retrieving of useful information.

As a record of each member's fields of interest is in our file, appropriate data can be expedited to where they may be needed. "Uniterm" type and punch card systems, and ultimately computers will aid in the retrieving process.

Until the system is fully organized, members will receive, periodically, bibliographies of current literature in the Research Service Center library of AFASE. The most important of these papers will be abstracted for the Journal.

Your suggestions for further improvements will be welcomed by the director of The Technical Research Service Center.

Hirt, R. C.; Schmitt, R. G.; Searle, N. D.; and Sullivan, A. P. "Ultraviolet Spectral Energy Distributions of Natural Sunlight and Accelerated Test Light Sources". *Journal of the Optical Society of America*, Vol. 50, No. 7, 706–713, July, 1960.

A contributory factor to the failure of correlation between outdoor and indoor photodecomposition tests is the difference in the ultraviolet spectral energy distributions of natural sunlight and the various indoor test sources which do not duplicate sunlight and differ widely among themselves. The ultraviolet spectral energy distributions of natural sunlight and of a variety of indoor exposure test sources have been measured. By use of a ferrioxalate actinometer, the measurements have been put on an absolute basis permitting the intercomparison of the sources. The xenon arc was found to be the best approximation of sunlight in the ultraviolet. For shorter-wavelength ultraviolet (below 3500 A), the combination of fluorescent Sunlamp and Blacklight lamps also approximated sunlight.

* * *

Hutchinson, F. W. *Nuclear Radiation Engineering*, The Ronald Press Company, New York, 155 pages.

The book is intended for the non-specialist who is engaged in activities requiring a general view of nuclear radiation and serves "as the equivalent of a language primer—as a means of improving understanding between the executive and the atomic scientist or nuclear engineer . . .". The book deals primarily not with nuclear reactor engineering, but with nuclear radiation engineering which involves a knowledge of the atomic and nuclear causes of radioactivity, the kinds of radioactivity, the energy release associated with the process of radioactive disintegration and, most emphatically, the effects of radiation. The subjects are divided into: 1 Atomic and Nuclear Structure; 2 Atomic and Nuclear Energy; 3 Radiation Absorption and Measurement; 4 Dictionary of Atomic and Nuclear Terms and Phrases.

* * *

Lansdell, N. *The Atom and the Energy Revolution.* Philosophical Library, 1958, 200 pages.

Divided into eight sections, an account is given of world energy resources and demand with particular emphasis on atomic energy. Section II, "New Sources of Energy" contains a brief statement (Pp 36–39) on Solar Energy. The Bell Laboratories solar battery is discussed as the beginning of a larger source of electrical energy derived from the sun. This book is not concerned primarily with research on the application of atomic energy or with the medical, industrial and agricultural uses of radioactive isotypes. The book is addressed, "To the specialist in respect of discipline other than his own: to the business man who must accommodate himself to the new industrial and commercial factors introduced by atomic energy . . .".

* * *

Heidt, L. J.; Livingston, R. S.; Rabinowitch, E.; and Daniels, Farrington. *Photochemistry in the Liquid and Solid States.* John Wiley and Sons, Inc., New York and London, 1960, 174 pages.

The availability of sunlight, the various ways in which it might be used photochemically, the limitations, and the ground rules for scientists and inventors are suggested in an introductory chapter. Following are chapters on Photochemical Reactions, Photosensitized Reactions, Fluorescence, Kinetic Considerations, Role of the Triplet State, Photochemical Reactions Involving Chlorophyll, Photoreactions in Solids, and a conclusion. The authors present the basic principles of photochemistry storage, survey the field of photochemical reactions, and state the requirements for reaction types which might prove useful for storing solar energy. This book also presents basic research findings and suggests the areas for further research which can lead to the use of the sun as an important and inexpensive source of energy.

* * *

Kopal, Zdenek. *Figures of Equilibrium of Celestial Bodies.* The University of Wisconsin Press, 1960, 135 pages.

The book emphasizes problems of motion of artificial satellites. The principal aim is to investigate mathematically the figures of equilibrium of selfgravitating compressible fluids and to specify the external form a gravitational potential of a fluid mass, initially spherical, subject to a given disturbing force, takes. The approach to this problem is that initially proposed by Clairaut in the 18th century. It is concerned with the construction of explicit expressions for the potential of a configuration. Following an introduction, the book is divided into First Order Theory, including iterative solutions of Clairaut's equations; Second Order Theory, including discus-

sion on surface form and exterior potential; Interaction Phenomena, e.g. between rotation and tides; and non-radical oscillations of self-gravitating fluids, and for stellar models of all evolutionary stages.

* * *

Kaye, J. and Welsh, J. A. *Direct Conversion of Heat to Electricity*. John Wiley and Sons, Inc., 1960.

A unique work in a field for which there is a great demand for organized information. As stated in the preface—"no single or concentrated source of reference material exists today to aid new workers in this field to gain a foothold on the varied theories and concepts involved." The papers of which this volume consists were presented at a special Summer Program offered by the Department of Mechanical Engineering of M. I. T. from July 6 to 17, 1959. The book is divided into five general areas: Thermionic Engines-High Vacuum; Thermionic Engines-Low Pressure; Magnetohydro Dynamic Converters; Semi-conductor Devices; Fuel Cells.

* * *

Coulson, K. L.; Dave, J. V.; and Sekera, Z. *Tables Related to Radiation Emerging from a Planetary Atmosphere with Rayleigh Scattering*, University of California Press, Berkeley and Los Angeles.

The book provides tables giving the exact distribution and polarization of reflected and transmitted light in a plane-parallel atmosphere scattering according to Rayleigh's laws and makes possible the determination by subtraction (from the observed distributions) the nonmolecular component of skylight. The foremost problem of radiative transfer in a sunlit planetary atmosphere is to determine the intensity and the polarization of the diffuse radiation emerging from the top and from the bottom of the atmosphere. The exact solution of this problem has been derived in an ingenious way by S. Chandrasekhar for the case of a plane-parallel atmosphere with Rayleigh scattering. This problem can be expressed in terms of four pairs of the so-called X and Y functions, satisfying four pairs of simultaneous, nonlinear integral equations, which can be solved by successive approximations. The solution of these integral equations has been carried out independently at the Watson Scientific Computing Laboratory in New York and at the Institute for Numerical Analysis of the National Bureau of Standards located on the campus of the University of California, Los Angeles. From these X and Y functions the Stokes parameters of the radiation emerging in different directions from the top and from the bottom of the atmosphere can be computed for different sun elevations and for different reflectivities of the ground. The results of the computations performed at the Western Data Processing Center at the University of California, Los Angeles are also included.

* * *

Ioffe, A. F. *Semiconductor Thermoelements and Thermoelectric Cooling*. Infosearch Limited, London, 1957, 184 pages.

An English translation of a Russian work which continues the studies first published in 1949 and supplemented in 1956. The discussion involves the general physical concepts of the construction and technology of thermoelectric batteries for specific purposes. The second chapter, "Experimental Investigation of the Thermoelectric Properties of Semi-conductors," according to the author, forms the core of the book. The first (introductory) chapter and the third (supplementary) chapter present, in an abbreviated form, previously published information.

* * *

Building Research Institute. "New Methods of Heating Buildings," Publication 760, National Academy of Sciences-National Research Council, 1960, 148 pages.

Friend, Walter F. and Jordan, A. Leo, Ebasco Services, Inc.

The authors predict adequate supplies of fuel and energy for the U. S. and its economic allies at least for the next decade and perhaps longer, and that with further research on the technical and commercial feasibility of the use of solar radiation and nuclear energy, a substantial part of the remaining fossil fuel reserves can be used in the future as basic raw material in the chemical industries. The paper considers solid fossil fuels, petroleum, natural gas, liquified petroleum gas, solar energy, nuclear fuels and geothermal energy in terms of current and future reserves, use in various types of systems, etc. Theoretical studies of the possibilities of using the force of gravity to produce power and heat are described, as well as of tidal power, water power and the so-called exotic fuels. Direct energy conversion to produce "fuel cells" directly from the chemical energy contained in fuels, without passing through the intermediate thermal and mechanical phases of conventional power cycles is discussed, accompanied by a table of Basic Principles and Definitions. The present status of electronic power transmission is mentioned, although it is noted that this appears still too far in the future to be of concern to the building industry at this time.

* * *

Gilkey, Herbert T., National Warm Air Heating and Air Conditioning Association

Attention is called to the fact that providing comfort in a space during a period of time must of necessity include cooling as well as heating, and that the term "air conditioning" is applicable equally to both processes. A major break-through which will result in totally new designs using new materials and techniques is predicted for the near future. New methods of producing catalytic combustion with gaseous fuels and new types of thermocatalytic reactors of ceramic materials are discussed, as well as thermionic converters involving electron emission from metals at high temperatures. New oil heating devices are described, and also the use of the heat pump and electric resistance heating as the heat source for an air system. Changes in control components and systems are noted including control of air cleanliness, humidity and moisture. Consideration is also given to use of new materials for ducts, advances in the use of supplying outlets, and the increasing variety of applications of the air heating system in apartment buildings, schools and commercial structures, several of which are discussed in detail. Attention is called to the outstanding growth of the use of perimeter heating for residences.

* * *

Lochkart, Harold A., Bell and Gossett Company. "Hydronic Heating".

This paper gives a brief history of steam and hot water heating, leading up to a full discussion of present-day methods. The use of smaller pipe sizes in hot water systems is predicted, with the advent of higher temperature drops. The new concept of parallel piping circuits, allowing the segmentation of the heating system is discussed. Designs for primary and secondary pumping systems are illustrated and described. Note is taken of the fact that temperatures are going up to a very high degree in today's practice of hydronic heating.

* * *

Carroll, J. Raymond, University of Illinois. "Radiant Systems for Heating."

The nature of radiant energy and its propagation are discussed, followed by an explanation of the nature of radiant energy exchange in terms of various heating systems. The effect of radiant heat on comfort, and the limitations of present methods for the measurement of comfort in an actual installation, are also considered. The author then analyzes radiant heating systems in three categories: low temperature, medium temperature, high temperature and specular radiant heating produced by the incandescent systems. In predicting the future use of radiant heating systems for different types of building occupancy, the author suggests the possibility of such devices as small, high-intensity infra-red emitters mounted in walls or ceiling around large glass areas; electricity conductive films imbedded in or adhered to floors, walls and ceilings; electric

drapes for windows which would be similar to today's electric blankets; and even electric window glass for large glass areas.

* * *

Faust, Frank H., General Electric Company. "New Electric Heating Systems".

Technological developments in the use of electric heating are cited as responsible for the rapid growth and acceptance of this type of system during the past decade. The general and specific benefits and limitations of all types of heating and air-conditioning systems using electricity are presented, and the situations and locations wherein such systems should be applied are described. The economics of the use of electric systems in comparison with other types are analyzed. Electric resistance heating and electric heat pumps are discussed separately with the above considerations in view, and current trends in the development of such systems, as well as what can be expected in the immediate future, are cited.

* * *

Jordan, Richard C., University of Minnesota. "The Future of Solar Heating".

Despite the marginal economy of solar space heating today, this paper indicates that the future is relatively bright for the development of this means of heating buildings. The availability of solar energy and its proportionate distribution by area throughout the country are described and illustrated. Various means of solar energy storage are enumerated and a table given to show heat storage capacity of various working media. Architectural considerations involved, along with different systems of solar heating, are discussed, and five individual buildings in which solar heating systems are now being employed are examined in detail. The author points to the use of solar energy as a heat source for heat pump systems as one of the most promising possibilities for developments which may involve energy storage in forms other than heat; i.e., through electrical, inertial, gas compression, chemical reaction or biological systems, or by the use of closed-cycle fuel cells.

* * *

Coulson, K. L.; Dave, J. V.; and Sekera, Z. *Tables Related to Radiation Emerging from a Planetary Atmosphere with Rayleigh Scattering*. University of California Press, Berkeley and Los Angeles

* * *

Penrod, E. B. and Prasanna, K. V. "Will Solar Energy be the Heat Source for Tomorrow's Heat Pump?". *Heating, Piping & Air Conditioning*, May 1960, Pp. 117–127.

An investigation has been made at the University of Kentucky in which the solar energy incident on a solar collector has been used as a heat pump source to supplement that stored in the earth's crust. A collector and ground coil supplied the evaporator load during the heating period, and the soil adjacent to the ground coil served as a reservoir for temporarily storing excess solar energy accumulated during bright sunny days. Due to the unpredictable nature of solar radiation and the lack of knowledge of the variation of the physical properties of the soil, calculations were based on monthly average values. A relative cost of operation of the system is also included. Actual operation of the heat pump system is limited to the assumptions made and to the capability of the machine to follow heating load fluctuations.

* * *

Poncelet, Eugene F., and Thuman, William C. "The Solar Furnaces of the Laboratoire de L'energie Solaire at Montlouis France," SRI Project No. 1621–531, 85 pages.

The status of the laboratory furnaces, the 60-Kw furnace, and the proposed "production plant" of the Solar Energy Laboratory at Montlouis was investigated. The development and the status of the processes evolved with these installations were evaluated, and the novel features of the Montlouis Plant were appraised. Conclusions drawn from the information detailed in the following sections are given in section VII.

* * *

Acker, Roy M.; Lipkis, Robert P.; Miller, Raymond S.; and Robison, Paul C. "Solar-Cell Power Supplies for Satellites," *Electronics*, March 11, 1960, Pp. 167–173.

For reliability in the space environment, silicon solar cells are proving their worth. In this article, basic design considerations are treated with details of their applications to the Able-4 Atlas space probes.

* * *

Bjorksten Research Laboratories, Incorporated. "Weathering Tests of Plastics and Design of Suspended Envelope Solar Stills," Research and Development Progress Report No. 30, Under contract no. 14-01-001-91, 40 pages, September 1959.

This is one of a series of reports designed to present accounts of progress on saline water conversion with the expectation that the exchange of such data will contribute to the development of economical processes applicable to large-scale, low-cost demineralization of sea or other saline water. Except for editing, the data herein are as contained in the final report submitted July, 1958 and revised May–August, 1959, by Bjorksten Research Laboratories, Inc., under Contract No. 14-01-001-91. Risto P. Lappala, project engineer, and L. L. Yeager, project engineer, were in charge of investigations for the Contractor. The data and conclusions given in this report are essentially those of the Contractor and are not necessarily endorsed by the Department of the Interior.

* * *

Calmpitt, Bert H. and German, Dale E. "Solar-to-Electric Energy", *SAE Journal*, May 1960, Pp. 52–55.

New two-stage device for converting solar energy into electrical energy promises operating efficiencies comparable with current photovoltaic devices and acts as its own storage battery. First stage will convert solar to chemical energy by the photochemical isomerization of trans to cis organic acids. (Cis and trans indicate two forms of geometrical isomers.) The next stage converts chemical to electrical energy by means of electrochemical concentration cells. Concentration cells using cis and trans acids have been constructed, and potentials approaching the theoretical value of about 0.1 v were measured. Maximum electrical power measured in the various systems was 2–3 microwatts per sq cm of electrode area, despite high internal resistances. Techniques for reducing these resistances are being investigated.

* * *

Schekin, V. "Solar Batteries," translation by B. W. Kuvshinoff, Library Bulletin, TG 230T65, April 17, 1959, 7 pages.

The emf attainable with silicon p-n elements is discussed. Use of silicon elements with buffer storage cells in telephone systems and miniature receivers is mentioned. Requirements for supplying house power by silicon photocells are calculated.

* * *

RCA News. "Rocket's Exhaust Heat is Turned to Electric Power in New Technique Announced by RCA and Thiokol", RCA News, Released November 24, 1959, 4 pages.

Light-weight thermionic tube mounted on rocket flame pipe produces current to operate steering mechanism and electronic apparatus.

Marcus, Rudolph J., and Wohlers, Henry C. "Photochemistry in the Solar Furnace", Reprinted from *Industrial and Engineering Chemistry*, Vol. 51, November 1959, Pp. 1335–1339.

The focal spot of the solar furnace can be used as a cool, intense light source. This use of the solar furnace can become important when it is desired to drive inherently inefficient photochemical reactions in the visible light range. Liquids as well as gases can be handled at the focus of the solar furnace as they absorb only selected wave lengths. The stoichiometry and kinetics of the photoreduction of ceric ion in perchloric acid solution remained unchanged in the solar furnace from those observed at room temperature and with artificial light sources.

* * *

Luft, Werner, and Nash, Harry. "Temperature Control of Silicon Solar Cells in Space Environment," *Semi-Conductor Products*, June 1960, Pp. 39–44.

The performance of silicon cells in converting radiant energy into electrical energy is dependent on the cell temperature. Most effected by temperature is the optimum power transfer characteristic, which has a temperature coefficient of $-.6\%$ per degree centigrade. In a space environment the temperature of a solar collector is determined by the radiation equilibrium and hence by the optical characteristics of its surface. Conventional silicon solar cells have optical characteristics which produce higher surface temperatures than desired for good operating efficiency. Optical coatings have been developed which notably reduce the temperature, with corresponding increase in power output.

* * *

Peet, C. S. *Semiconductor Abstracts*, Vol. V, 1957 issue John Wiley and Sons, Incorporated, London, 449 pages.

Sponsored by the Electrochemical Society, Inc. and compiled by Battelle Memorial Institute with C. S. Peet as editor to this 1957 issue is a continuation of abstract publications begun in 1953. The problem of condensation has resulted in the omission of some of the kinds of material offered in previous issues. Solid-state phenomena of lesser relevance to semiconductor interests, such as perovskite ferromegenetics and organic ferroelectrics and fringe phenomena such as solution luminescence and single-atom emissions have been omitted. The abstracts are cross referenced and divided into Elemental Semiconductors and Compound Semiconductors. A section on Theory contains 44 abstracts. The Section on General Applications, consisting of 101 abstracts includes Junctions, Contacts, Rectifiers, and Electrons; Transistors, Diodes, Triodes, and Texodes; Cathodes, and Oxide-coated Cathodes; Miscellaneous Applications.

* * *

Upjohn Company. *Psoralens and Radiant Energy*, Vol. 32, Feb. 1959, No. 2. (supplement to *The Journal of Investigative Dermatology*), 254 pages.

The furocoumarin compounds and their effects on melanin pigmentation are presented in a series of papers which were presented at the Brook Lodge Invitational Symposium on the Psoralens, sponsored by the Upjohn Company, March 27–28, 1958. The Symposium includes the field of radiation physics, the chemical make-up of some compounds affecting pigment, hormonal factors causing increased or decreased pigmentation, and the clinical uses of chemical, hormonal, and physical agents in human subjects.

* * *

Adolphe, E. F. *Physiology of Man in the Desert*. Interscience Publishers, Incorporated, New York, 1947, 357 pages.

A series of monographs carrying summaries of data collected by the University of Rochester under contract from the U. S. Office of Scientific Research and Development on "problems which must be met if American soldiers were called upon to conduct a war on or over the desert of North Africa . . . The data contained in these reports bearing on health and survival in the desert are no less applicable to civilians who reside or have occasion to travel the land of high temperatures and little rainfall than to the military . . ." The purpose of the book is to solve the problems of maintaining efficiency in the desert, a matter of long temperature regulation. Much of the discussion is concerned with water and heat metabolism.

Abstracts of American Rocket Society papers relating to solar energy presented at the American Rocket Society Space Power Systems Conference, Santa Monica, California, September 27–30, 1960. (ARS preprint number of each paper is shown in parentheses)

Loferski, J. J. "The Photovoltaic Effect and Solar Energy Conversion," (ARS 1288–60).

The general equations which describe the photovoltaic effect as a means of energy conversion will be presented. Based on the equations, it has been inferred that there exist semiconductors whose maximum solar energy conversion efficiency could be even higher than that of silicon. Experimental investigations of such materials has led to a maximum solar energy conversion efficiency somewhat higher than 7% in GaAs and CdS and lower values in CdTe, InP, and others. Analysis of spectral response of cells made from these materials is being used to direct further experiments aimed at increasing these efficiencies. The potential advantage of such materials for higher temperature operation such as that which will probably result from light concentration will be evaluated. Studies of radiation damage produced in silicon and gallium arsenide by radiations like those encountered in space will also be discussed.

* * *

Middleton, A. E.; Gorski, D. A.; Shirland, F. A. "Evaporated CdS Film Photovoltaic Cells for Solar Energy Conversion," (ARS 1291–60).

Replacement of the semiconducting single crystal slab in solar cells by a deposited macrocrystalline film or layer can lead to major advances in solar battery utilization, design and cost, and weight reduction. Significant progress toward these objectives has been made with CdS. CdS films up to 0.2 mm in thickness have been vacuum evaporated on various heated substrates. Films formed from purified and doped CdS single crystal chips are macrocrystalline and have resistivities less than 1 ohm-cm with good optical transmission. Back wall solar cells have been made from such films deposited on conducting tin oxide coated glass employing the same barrier forming process as used on single crystal CdS cells. Direct sunlight conversion efficiencies of up to 3.5% have been achieved.

* * *

Stone, L. E.; Powderly, J. E.; Medcalf, W. E. "Integrally Composed Variable Energy Gap Photovoltaic Cells," (ARS 1292-60).

Progress in the fabrication and preparation of integrally composed variable gap gallium arsenide-gallium phosphide photovoltaic cells is discussed. The front surface of the variable gap cell facing the incident light represents the region (GaP) of greatest band gap, and the rear section (GaAs) farthest from the incident light is the region of the lowest band gap. The transition area between these two regions is composed of $Ga(As_x\ P_{1-x})$ and contains the p $-$ n junction. Significant

differences of photoparameters compared to single gap gallium arsenide cells were noted. Short circuit current, open circuit voltage, conversion efficiencies, and dark diode characteristics of gallium arsenide photovoltaic cells were consistently improved by the controlled in-diffusion of phosphorus to provide an area of variable band gap.

* * *

Evans, W. H.; Mann, A. E.; Wright, W. V., Jr., "Solar Panel Design Considerations," (ARS 1296-60).

The requirements and parameters of photovoltaic solar array design for space applications are presented. Orbit conditions of insolance, electrical power requirements and panel geometry are discussed. The relation of solar cell spectral response, surface spectral characteristics and temperature control is presented and the use of spectrally selective surfaces is examined. The effects of electrical circuit design and space environment on reliability is also briefly discussed.

* * *

Thelen, Alfred, "The Use of Vacuum Deposited Coatings to Improve the Conversion Efficiency of Silicon Solar Cells in Space," (ARS 1298-60).

The conversion efficiency of silicon solar cells decreases rapidly with increasing cell temperature. Since the emission characteristics of bare silicon solar cells are rather poor, the bare cells stabilize in a radiation equilibrium with the sun at an efficiency decreasing high temperature. Vacuum deposited coatings help to improve the absorption and emission characteristics of silicon solar cells. For various space applications the influence of several types of coatings on the conversion efficiency of silicon solar cells is shown. The merits of coated glass covers versus direct coatings on the cells is discussed. Details will be given of new developments such as commercially available near IR reflecting coatings and selectively reflecting coatings for collector mirrors. Finally, certain limitation in the application of vacuum deposited coatings are pointed out and discussed.

* * *

Purdy, David L. "Solar Thermionic Electric Power System," (ARS 1311-60).

The theoretical application of vacuum type thermionic converters for a space power supply utilizing solar power is discussed. The characteristics of presently available, commercially produced thermionic converters are described, and the integration of these characteristics, with those of other system components, is explained. Particular emphasis is placed on the importance of the solar concentrator. A specific "Solar Thermionic Electric Power System" is described. This system is composed of a reflecting energy concentrator of an automatically unfolding design driven by an orientation sub-system of silicon sensors and mechanical drive elements. At the focus of this concentrator, a thermal to electrical power converter, or generator, is placed. Thermionic converter elements form the basic component of this generator. Electrical energy storage for operating during the dark portion of a satellite orbit will be provided, and a regulation sub-system regulates the voltage between 26 and 29 volts. The report describes hardware development in progress on this system.

* * *

Henderson, R. E.; Dresser, D. L. "Solar Concentration Associated with the Stirling Engine," (ARS 1312-60).

Progress in the development of a lightweight solar concentrator for the Stirling engine power system is reviewed. The preliminary study activity which led to the selection of an all-metal Fresnel reflector component is given. Reasons for choosing the Fresnel configuration are listed. The optical performance of the modified Fresnel reflector is presented—this includes the ideal intensity distribution, the lost area factor, and some estimated solar collector efficiencies for both the Stirling engine application and a thermionic system. The electroforming fabrication approach which is being developed is described. Finally, experimental results from two 40.6 cm diameter model reflectors are evaluated for the concentration performance.

* * *

McClelland, Donald H. "Solar Concentrators for High Temperature Space Power Systems," (ARS 1314-60).

Basic problems in the development of lightweight, high efficiency, solar concentrating mirrors for space power systems are discussed. Various concentrator and absorber configurations are compared both on the basis of idealized performance and in regard to performance degradation due to geometric errors. Concentrator structural design classifications are presented and are related to fabrication techniques, materials, and reflective surfacing methods. Orientation requirements and the effects of the space environment are considered. Tests are presented for determining collector performance and for evaluating mirror surface quality.

* * *

Rudy, James A. "Sunflower Power Conversion System," (ARS 1349-60).

Sunflower is a solar power conversion system being developed by Thompson Ramo Wooldridge Inc. under contract to The National Aeronautics and Space Administration. The contract effort was initiated on June 1, 1960, and the currently contracted development program is to be completed April 1, 1964. This paper describes the proposed Sunflower System, defines the bases on which it has been conceived, and establishes the relationship of the Sunflower System requirements with the state of the art of today's power conversion system development.